
CHE-TKG: Collaborative Historical Evidence and Evolutionary Dynamics Learning for Temporal Knowledge Graph Reasoning

Shuai-long Lei, Xiaobin Zhu*, Jiarui Liang, Guoxi Sun, Zhiyu Fang, Xu-Cheng Yin

University of Science and Technology Beijing

shuailong01ei@gmail.com, zhuxiaobin@ustb.edu.cn, m202510664@xs.ustb.edu.cn

sgxxyds@foxmail.com, mr.fangzy@foxmail.com, xuchengyin@ustb.edu.cn

Abstract

Temporal knowledge graph (TKG) reasoning aims to predict future events from historical facts. A key challenge lies in jointly capturing two sources of predictive information in TKGs: historical evidence and evolutionary dynamics. However, existing methods typically focus on only one of these sources, which limits the ability to fully exploit the complementary predictive signals in TKGs. To address this, we propose CHE-TKG, a novel collaborative dual-view learning framework for TKG reasoning. CHE-TKG explicitly separates and jointly models historical evidence and evolutionary dynamics, aiming to learn and exploit their complementary predictive signals. Specifically, CHE-TKG constructs a historical evidence graph to capture long-term structural regularities and stable relational constraints, alongside an evolutionary dynamics graph to model temporal transitions and recent changes, with dedicated encoders for each view. We further employ relation decomposition and a contrastive alignment objective to better capture the predictive signals across the two views. Extensive experiments demonstrate that CHE-TKG achieves state-of-the-art performance on multiple benchmarks.

1 Introduction

Temporal knowledge graphs (TKGs) model real-world facts with temporal information, where each fact is represented as a quadruple (*subject, relation, object, timestamp*) and organized as a sequence of time-ordered snapshots. This temporal modeling supports a wide range of downstream applications, such as recommendation [42, 47], question answering [1, 34], and information retrieval [50, 11]. Due to the inherent incompleteness of TKGs [54, 13, 9, 31], temporal knowledge graph reasoning (TKGR) aims to infer missing facts at specific timestamps.

TKGs often exhibit two distinct sources of predictive information [36, 20, 7], namely historical evidence (E) and evolutionary dynamics (D), which may provide complementary predictive signals for TKGR. Complementary predictive signals refer to different yet useful predictive cues captured from these two sources. Recent TKGR methods attempt to leverage structural inductive biases to capture these two aspects, as shown in Fig. 1(b). One line of work [27, 9, 52, 54] focuses on historical evidence, where historically observed relevant events are aggregated while discarding temporal information. Another line of research [13, 8] emphasizes evolutionary dynamics, typically leveraging various mechanisms to model temporally ordered events, thereby capturing time-evolving dependencies. However, these methods typically focus on only one of these sources, which limits the ability to fully exploit the complementary predictive signals in TKGs.

To better understand these two aspects, we instantiate them as two graph structures in a TKG: a historical evidence graph and an evolutionary dynamics graph. Fig. 1(a) illustrates this construction

*Corresponding Author

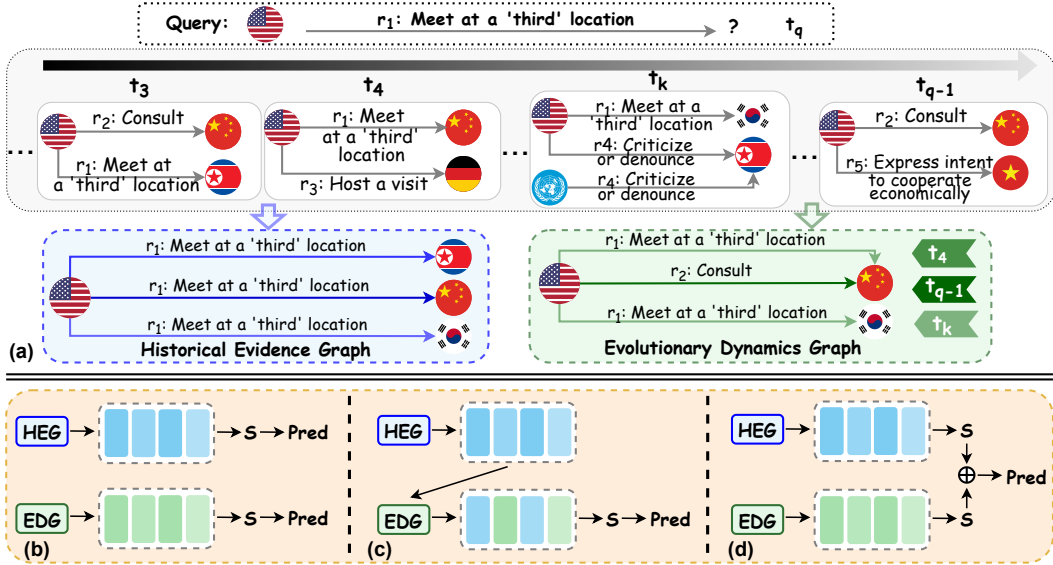


Figure 1: An illustrative example of the two views, including graph construction on the ICEWS dataset and comparisons of different reasoning paradigms. (a) Construction of a historical evidence graph and an evolutionary dynamics graph from the observed TKG given a query. (b) Single-view reasoning paradigm. After obtaining entity and relation embeddings, prediction is performed by computing scores. (c) Naive joint modeling of both views. (d) Our CHE-TKG with explicit separation and joint learning of two views.

using an example from the ICEWS dataset. Given the query $q = (\text{North America}, \text{Meet at a 'third' location}, ?, t_q)$, historical facts of the form $(\text{North America}, \text{Meet at a 'third' location}, e_o, t)$ with $t < t_q$ reflect accumulated historical evidence. Removing timestamps and aggregating these facts corresponds to a historical evidence graph (blue dashed region), which captures long-term structural regularities and stable relational constraints. In parallel, logically related recent events, derived from temporal logical rules [35], capture the evolutionary dynamics, which can be organized as an evolutionary dynamics graph (green dashed region) to capture query-relevant temporal transitions. Although naively combining these two structures enables joint learning, such integration still poses a significant challenge, as shown in Fig. 1(c). In particular, simple joint modeling may suffer from shortcut learning, where the model tends to favor easier-to-learn patterns while failing to preserve informative signals [38, 39]. As a result, complementary predictive signals may be under-utilized or collapsed in the learned representations, preventing them from being fully exploited.

To address the aforementioned challenges, we propose CHE-TKG, a novel collaborative dual-view learning framework for TKGR. CHE-TKG explicitly separates and jointly models historical evidence and evolutionary dynamics through two dedicated structural views, thereby better learning and exploiting complementary predictive signals, as shown in Fig. 1(d). Specifically, we construct a historical evidence graph and an evolutionary dynamics graph, and employ two dedicated encoders to learn view-specific representations. The historical evidence graph captures long-term structural regularities and stable relational constraints, while the evolutionary dynamics graph models temporal transitions and recent changes. We also incorporate relation decomposition to learn view-specific relation semantics, and introduce contrastive alignment to encourage the two views to capture task-relevant signals. Our main contributions are summarized as follows:

- We propose a novel collaborative dual-view learning framework for TKGR (dubbed CHE-TKG) to better learn and exploit complementary predictive signals from historical evidence and evolutionary dynamics.
- We construct historical evidence and evolutionary dynamics graphs with dedicated encoders, and introduce relation decomposition and contrastive alignment to learn view-specific semantics and task-relevant cross-view signals.
- We theoretically show that the collaborative dual-view learning framework can improve ranking reliability by reducing pair-level ranking errors under mild conditions.

- Extensive experiments on multiple benchmark datasets verify that CHE-TKG consistently achieves state-of-the-art performance in extrapolation settings.

2 Related Work

Since TKGs are inherently graph-structured, many extrapolation reasoning methods adopt graph neural networks (GNNs) to learn entity and relation embeddings. RE-NET [19] and RE-GCN [30] pioneered the paradigm by modeling spatial structures with GNNs and capturing local temporal context across snapshots using recurrent neural networks (RNNs). Building upon this paradigm, subsequent works explore two main directions. Some approaches focus on relation-centric modeling to improve entity representations [5, 55, 33, 31], while others [29, 28, 41] strengthen temporal modeling across recent snapshots through various designs. However, these methods do not explicitly instantiate historical evidence or evolutionary dynamics as dedicated structural views.

Recent approaches attempt to explicitly model either historical evidence or evolutionary dynamics by introducing extra graph structures. Specifically, HGLS [56] builds a global graph over a large temporal window, while DyMemR [52] maintains a memory pool to selectively store global historical information. TiRGN [27] introduces a global historical replay matrix, whereas LogCL [9] and HisRES [54] model global two-hop and one-hop historical dependencies, respectively. These approaches primarily leverage query-related, time-agnostic global structures to model historical evidence, improving the utilization of long-term contextual information. Meanwhile, another line of work emphasizes temporal evolution through dynamic structures. For instance, HERLN [13] combines Hawkes processes with structural properties such as community and long-tail distributions, and HTCCN [8] adopts causal convolutions and Hawkes processes to capture temporal dependencies, temporal decay, and event intensities. However, existing approaches do not unify the modeling of historical evidence and evolutionary dynamics, leaving a gap in jointly modeling and leveraging the complementary predictive signals from the two sources. Further details on other TKGR methods can be found in Appendix A.

3 Methodology

3.1 Preliminaries

Task Definition. A temporal knowledge graph (TKG) is defined as $(\mathcal{E}, \mathcal{R}, \mathcal{T}, \mathcal{F})$, where \mathcal{E} , \mathcal{R} , \mathcal{T} , and \mathcal{F} denote the sets of entities, relations, timestamps, and temporal facts, respectively. Each fact $f \in \mathcal{F}$ is a quadruple (e_s, r, e_o, t) with $e_s, e_o \in \mathcal{E}$, $r \in \mathcal{R}$, and $t \in \mathcal{T}$. Facts are organized into time-ordered snapshots $\mathcal{G} = \{\mathcal{G}_1, \mathcal{G}_2, \dots\}$, where $\mathcal{G}_t = \{(e_s, r, e_o, t) \mid (e_s, r, e_o, t) \in \mathcal{F}\}$. Extrapolation reasoning aims to infer facts at unseen future timestamps and is formulated as a link prediction task that answers queries $q = (e_s, r, ?, t_q)$. During training, only historical facts with $t_i < t_q$ are observable, while facts at timestamp t_q and beyond remain unobserved. We denote by \mathcal{Q}_{t_q} the set of such queries at timestamp t_q . Following prior work, inverse relations are introduced by adding edges (e_o, r^{-1}, e_s, t) , allowing subject prediction queries to be transformed into tail prediction queries. For simplicity, we describe the task in terms of tail entity prediction in the subsequent analysis. A summary of important notations is provided in Appendix B.

Temporal Logical Rule. A temporal logical rule \mathcal{TR} is defined as $(A, r_h, B, t_2) \leftarrow (A, r_b, B, t_1)$, $t_2 > t_1$, indicating that the occurrence of relation r_b between entities A and B at time t_1 supports the occurrence of relation r_h between the same entities at a later time t_2 . The confidence of a rule is measured by how often the rule body is followed by the rule head.

3.2 Framework

We propose a collaborative dual-view learning framework CHE-TKG for TKGR, as illustrated in Fig. 2. CHE-TKG constructs a historical evidence graph and an evolutionary dynamics graph from observed facts to model two complementary sources of predictive information. The historical evidence graph captures long-term structural regularities and stable relational patterns, while the evolutionary dynamics graph captures recent temporal transitions and time-sensitive changes. Facts from recent snapshots are incorporated to initialize spatio-temporal entity and relation representations, providing general contextual information for subsequent collaborative reasoning. After initialization, relation

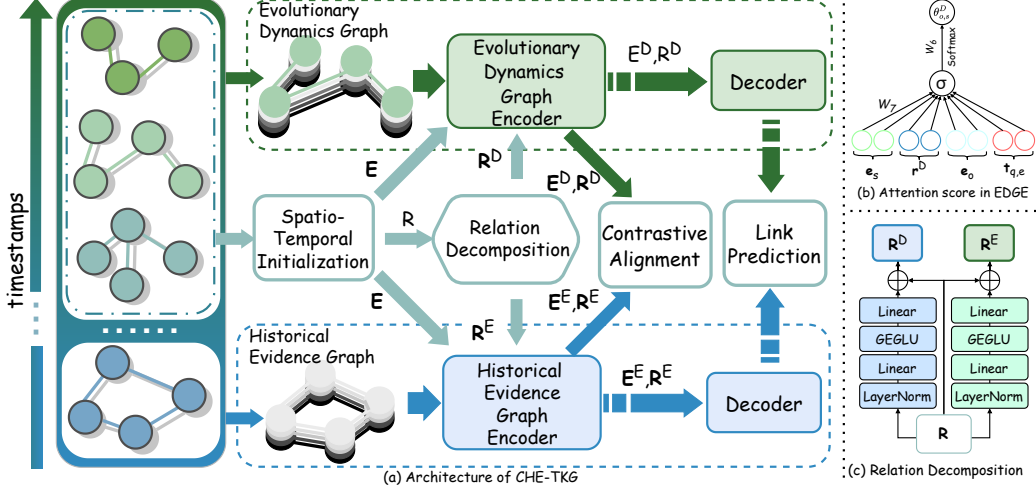


Figure 2: Overall architecture of CHE-TKG (a). The framework consists of spatio-temporal initialization, relation decomposition (c), a historical evidence graph encoder, and an evolutionary dynamics graph encoder with time-aware attention scores (b), followed by contrastive alignment.

representations are decomposed into view-specific components, enabling a relation to carry different semantics in the historical and evolutionary views. Then, the Historical Evidence Graph Encoder (HEGE) and Evolutionary Dynamics Graph Encoder (EDGE) encode the decomposed relations and entity embeddings to learn view-specific structural signals from the two graphs. A contrastive alignment mechanism further aligns query representations across views to promote task-relevant complementarity. Finally, the dual-view representations are combined in the decoder for entity prediction, allowing CHE-TKG to exploit complementary predictive signals from both views.

3.3 Collaborative Graph Construction

Historical Evidence Graph. We construct the historical evidence graph by aggregating historical events while discarding explicit temporal information. Specifically, given a query $q = (e_s, r, ?, t_q)$, we retrieve all historical facts $f_{t_q}^E = (e_s, r, e_o, t)$ with $t < t_q$ and incorporate them into the corresponding historical evidence subgraph $G_{t_q}^E \in \mathcal{G}^E$. As t_q increases, the historical evidence graph and the evolutionary dynamics graph are constructed from an expanded set of historical facts observed prior to t_q . For each timestamp t_q , all facts associated with its queries are aggregated into the same historical evidence and evolutionary dynamics subgraphs, denoted as $G_{t_q}^E$ and $G_{t_q}^D$.

Evolutionary Dynamics Graph. We construct the evolutionary dynamics subgraph $G_{t_q}^D$ using a temporal logical rule-based retrieval strategy. Specifically, we first mine temporal logical rules using TLogic [35] and sort them by confidence in descending order. Given a query $q = (e_s, r, ?, t_q)$, the query relation r is treated as the head relation r_h , and rules with head relation r_h are selected accordingly. For each selected rule with body relation r_b , we retrieve historical facts of the form $f_{t_q}^D = (e_s, r_b, e_b, t)$ with $t < t_q$ in reverse chronological order, where e_b denotes an entity connected to e_s via the rule body relation. These facts are then incorporated into $G_{t_q}^D$ until a predefined upper bound N is reached. For each edge, we explicitly encode the relative time interval $\Delta t = t_q - t$ as edge information, allowing the model to capture fine-grained temporal evolution patterns. Additional analysis of rule-based retrieval is provided in Appendix C.

3.4 Initialization

The initialization stage provides spatio-temporal representations by leveraging temporal and structural information from recent snapshots. Given the snapshot at time $t - 1$, we employ a graph convolutional network (GCN) to aggregate multi-relational neighborhood information within each snapshot:

$$\mathbf{e}_{o,t-1}^{l+1} = \sigma \left(\sum_{(e_s, r, e_o) \in \mathcal{G}_{t-1}} \frac{1}{c_o} W_1^l \kappa(\mathbf{e}_{s,t-1}^l, \mathbf{r}_{t-1}^l) + W_2^l \mathbf{e}_{o,t-1}^l \right), \quad (1)$$

where $\mathbf{e}_{s,t-1}^l$ and $\mathbf{e}_{o,t-1}^l$ are entity embeddings at time $t-1$ in the l -th layer, W_1^l and W_2^l are learnable parameters, c_o denotes the in-degree normalization factor, and $\sigma(\cdot)$ is the RReLU activation function. Following [54], relation embeddings are updated jointly in the GCN, and $\kappa(\cdot)$ denotes a one-dimensional convolution operator as in [27]. After modeling snapshot-level spatial structures with GCNs, we employ Gated Recurrent Units (GRUs) to capture temporal dependencies across snapshots. Specifically, the entity and relation representations are updated as:

$$\mathbf{E}_t = \text{GRU}_E(\mathbf{E}_{t-1}, \mathbf{E}_{t-1}^{\text{GCN}}), \quad \mathbf{R}_t = \text{GRU}_R(\mathbf{R}_{t-1}, \mathbf{R}'_t). \quad (2)$$

where \mathbf{E}_t and \mathbf{E}_{t-1} denote the entity embedding matrices at time steps t and $t-1$, $\mathbf{E}_{t-1}^{\text{GCN}}$ is the GCN output at time $t-1$, and \mathbf{R}'_t denotes the intermediate relation representation matrix. For each relation r , its intermediate representation is constructed as $\mathbf{r}'_t = [\text{pool}(\mathbf{E}_{r,t}) \parallel \mathbf{r}]$, where $\mathbf{E}_{r,t}$ denotes the embeddings of entities associated with relation r at time t , and $\text{pool}(\cdot)$ denotes mean pooling.

3.5 Relation Decomposition

To learn heterogeneous relational semantics and preserve view-specific predictive signals across the two graph views, we introduce a relation decomposition mechanism that learns view-specific relation representations. Formally, given a base relation embedding r , we derive the view-specific relation embedding for each view $v \in \{E, D\}$ via multiplicative modulation:

$$\hat{r}^v = (\mathbf{1} + g^v(r)) \odot r, \quad g^v(r) = W_3^v \text{Drop}(\text{GEGLU}(\text{LN}(r))), \quad v \in \{E, D\}. \quad (3)$$

where \hat{r}^E and \hat{r}^D are used in the historical evidence graph and the evolutionary dynamics graph, respectively, $\mathbf{1}$ denotes an all-ones vector, and \odot denotes element-wise multiplication. Here, W_3^v is a view-specific learnable projection matrix, $\text{LN}(\cdot)$ denotes layer normalization, $\text{GEGLU}(\cdot)$ [40] applies a gated linear unit with GELU activation, and $\text{Drop}(\cdot)$ denotes dropout.

3.6 Graph Encoder

To capture event correlations in both graphs, we adopt a Graph Attention Network (GAT) architecture with two view-specific encoders: the Historical Evidence Graph Encoder (HEGE) and the Evolutionary Dynamics Graph Encoder (EDGE). Entity and relation representations are initialized with spatio-temporal and decomposed embeddings, respectively. To model temporal relevance, we encode the relative time interval between the query $q = (e_s, r, ?, t_q)$ and a historical fact (e_s, r, e_o, t_e) as: $t_{q,e} = \Phi(t_q - t_e)$, where $\Phi(\cdot)$ follows TGAT [49]: $\Phi(t) = \sqrt{\frac{1}{d}} [\cos(w_1 t + p_1), \dots, \cos(w_d t + p_d)]$. The attention coefficients in the EDGE and HEGE are then defined as:

$$\theta_{o,s}^{D,l} = \frac{\exp(W_4^l \sigma(W_5^l [\mathbf{e}_s^l \parallel \hat{\mathbf{r}}^D \parallel \mathbf{e}_o^l \parallel t_{q,e}]))}{\sum_{(e_s, r') \in \mathcal{N}^D(o)} \exp(W_4^l \sigma(W_5^l [\mathbf{e}_s^l \parallel \hat{\mathbf{r}}^D \parallel \mathbf{e}_o^l \parallel t_{q,e'}]))}. \quad (4)$$

$$\theta_{o,s}^{E,l} = \frac{\exp(W_6^l \sigma(W_7^l [\mathbf{e}_s^l \parallel \hat{\mathbf{r}}^E \parallel \mathbf{e}_o^l]))}{\sum_{(e_s, r) \in \mathcal{N}^E(o)} \exp(W_6^l \sigma(W_7^l [\mathbf{e}_s^l \parallel \hat{\mathbf{r}}^E \parallel \mathbf{e}_o^l]))}. \quad (5)$$

For both graph views $v \in \{E, D\}$, entity representations are updated by:

$$\mathbf{e}_o^{v,l+1} = \sigma \left(\sum_{(e_s, r, e_o) \in \mathcal{G}_{t_q}^v} \theta_{o,s}^{v,l} W_8^{v,l} \psi(\mathbf{e}_s^{v,l} + \hat{\mathbf{r}}^{v,l}) + W_9^{v,l} \mathbf{e}_o^{v,l} \right), \quad (6)$$

where $\mathbf{e}_s^{v,l}$ and $\mathbf{e}_o^{v,l}$ denote the source and target entities' embeddings at layer l , $\hat{\mathbf{r}}^{v,l}$ denotes the decomposed relation embedding, $\mathcal{N}^v(o)$ denotes the incoming neighbors of e_o in graph view v , $W^{(\cdot)}$ are learnable parameters, $\psi(\cdot)$ denotes a 1-D convolution operator, and $\sigma(\cdot)$ is an activation function.

3.7 Contrastive Alignment

After encoding the two graph views with EDGE and HEGE, we obtain entity and relation representations from both graphs. Given a query $q = (e_s, r, ?, t_q) \in \mathcal{Q}_{t_q}$, we construct view-specific query representations and align them using an InfoNCE-based contrastive objective:

$$\mathbf{z}_q^v = \text{MLP}^v([\mathbf{e}_s^v \parallel \mathbf{r}^v]), \quad v \in \{D, E\},$$

$$\mathcal{L}_{D \rightarrow E} = -\mathbb{E}_{q \in \mathcal{Q}_{t_q}} \log \frac{\exp(\mathbf{z}_q^D \cdot \mathbf{z}_q^E / \gamma)}{\sum_{q' \in \mathcal{Q}_{t_q}} \exp(\mathbf{z}_q^D \cdot \mathbf{z}_{q'}^E / \gamma)}. \quad (7)$$

where MLP^v is implemented with an LN-GEGLU-Drop-Linear block with independent parameters, and γ is a temperature parameter. The final contrastive objective is defined symmetrically as $\mathcal{L}_{\text{CoA}} = \mathcal{L}_{D \rightarrow E} + \mathcal{L}_{E \rightarrow D}$, where $\mathcal{L}_{E \rightarrow D}$ is defined analogously. This contrastive alignment encourages the two views to capture task-relevant cross-view signals rather than task-irrelevant noise.

3.8 Prediction and Optimization

For link prediction, CHE-TKG adopts ConvTransE following [30, 9, 54] as the scoring function to compute the compatibility score between a query $(e_s, r, ?, t)$ and a candidate entity e_o . Given representations learned from the two graph views, the final prediction score is obtained by summing the view-specific scores:

$$f(e_o | e_s, r, t) = \sum_{v \in \{E, D\}} f^v(e_o | e_s, r, t), \quad f^v(e_o | e_s, r, t) = \text{ConvTransE}(\mathbf{e}_{s,t}^v, \mathbf{r}_t^v) \cdot \mathbf{e}_{o,t}^v. \quad (8)$$

where $\mathbf{e}_{s,t}^v$, \mathbf{r}_t^v , and $\mathbf{e}_{o,t}^v$ denote the subject entity, relation, and candidate object representations in view v , respectively. To enhance relation representations, we further introduce relation prediction as an auxiliary task. Let \mathcal{Q}_t^e and \mathcal{Q}_t^r denote the sets of entity and relation prediction queries at timestamp t , respectively. The task objective is defined as:

$$\mathcal{L}_{\text{TKG}} = \alpha \sum_{(e_s, r, e_o, t) \in \mathcal{Q}_t^e} \mathcal{L}_{\text{CE}}(e_o | e_s, r, t) + (1 - \alpha) \sum_{(e_s, r, e_o, t) \in \mathcal{Q}_t^r} \mathcal{L}_{\text{CE}}(r | e_s, e_o, t). \quad (9)$$

where $\mathcal{L}_{\text{CE}}(\cdot)$ denotes the cross-entropy loss, $\alpha \in [0, 1]$ balances entity and relation prediction tasks. Finally, the overall training objective combines the task loss with the contrastive alignment loss:

$$\mathcal{L} = \mathcal{L}_{\text{TKG}} + \mu \mathcal{L}_{\text{CoA}}, \quad (10)$$

where $\mu \geq 0$ controls the contribution of contrastive alignment.

3.9 Theoretical Analysis

Temporal knowledge graph reasoning under the extrapolation setting can be formulated as a ranking problem. Since CHE-TKG produces two view-specific scores from historical evidence and evolutionary dynamics, we analyze the corresponding pair-level score margins to understand when such dual-view signals improve ranking reliability. Given a query $q = (s, r, ?, t)$, the model aims to assign a higher score to the ground-truth entity o^+ than to a negative candidate o^- . For each query–negative pair (q, o^-) , ranking correctness is characterized by the margin:

$$\gamma(q, o^-) = S(q, o^+) - S(q, o^-), \quad (11)$$

where $\gamma(q, o^-) > 0$ indicates a correct ranking and $\gamma(q, o^-) \leq 0$ indicates a pairwise ranking error. Thus, increasing the ranking margin is crucial for improving ranking metrics.

CHE-TKG performs prediction from two views: the evolutionary dynamics view and the historical evidence view, which produce scores $S_D(q, o)$ and $S_E(q, o)$, respectively. The final score is obtained via score-level fusion, and the corresponding view-specific and fused margins are defined as:

$$\begin{aligned} S_{D+E}(q, o) &= S_D(q, o) + S_E(q, o), \\ \gamma_v(q, o^-) &= S_v(q, o^+) - S_v(q, o^-), \quad v \in \{D, E\}, \\ \gamma_{D+E}(q, o^-) &= S_{D+E}(q, o^+) - S_{D+E}(q, o^-). \end{aligned} \quad (12)$$

By score additivity, the fused margin satisfies:

$$\gamma_{D+E}(q, o^-) = \gamma_D(q, o^-) + \gamma_E(q, o^-). \quad (13)$$

This shows that score-level fusion aggregates ranking signals from both views. Intuitively, if the two views provide positive yet non-identical ranking signals, the fused margin is expected to increase to reduce pairwise ranking errors. We formalize this intuition through the following result. For analytical clarity, we suppose that the two margins follow identical Gaussian marginals, $\gamma_D, \gamma_E \sim \mathcal{N}(\mu, \sigma^2)$.

Table 1: Performance of TKG entity extrapolation on ICEWS14s, ICEWS18, ICEWS05-15 and GDEL T. The best results are marked in **bold**, and the second-best results are underlined.

| Model | ICEWS14s | | | ICEWS18 | | | ICEWS05-15 | | | GDEL T | | |
|----------------|--------------|--------------|--------------|--------------|--------------|--------------|--------------|--------------|--------------|--------------|--------------|--------------|
| | MRR | Hits@1 | Hits@10 | MRR | Hits@1 | Hits@10 | MRR | Hits@1 | Hits@10 | MRR | Hits@1 | Hits@10 |
| RE-NET | 36.93 | 26.83 | 54.78 | 29.78 | 19.73 | 48.46 | 43.67 | 33.55 | 62.72 | 19.55 | 12.38 | 34.00 |
| RE-GCN | 42.39 | 31.96 | 62.29 | 32.62 | 22.39 | 52.68 | 48.03 | 37.33 | 68.51 | 19.69 | 12.46 | 33.81 |
| RETIA | 42.76 | 32.28 | 62.75 | 32.43 | 22.23 | 52.94 | 47.26 | 36.64 | 67.76 | 20.12 | 12.76 | 34.49 |
| RPC | – | – | – | 34.91 | 24.34 | 55.89 | 51.14 | 39.47 | 71.75 | 22.41 | 14.42 | 38.33 |
| TANGO | 36.80 | 27.43 | 54.93 | 28.68 | 19.35 | 47.04 | 42.86 | 32.72 | 62.34 | 19.53 | 12.43 | 33.19 |
| HisMatch | 46.42 | 35.91 | 66.84 | 33.99 | 23.91 | 53.94 | 52.85 | 42.01 | 73.28 | 22.01 | 14.45 | 36.61 |
| CEN | 42.20 | 32.08 | 61.31 | 31.50 | 21.70 | 50.59 | 46.84 | 36.38 | 67.01 | 20.39 | 12.96 | 34.97 |
| HTCCN | 45.39 | 36.58 | – | 35.63 | 24.90 | – | 51.94 | 40.32 | – | 23.46 | 15.18 | – |
| HERLN | 43.94 | 34.62 | 63.44 | 31.33 | 21.93 | 52.01 | – | – | – | – | – | – |
| TiRGN | 44.75 | 34.26 | 65.28 | 33.66 | 23.19 | 54.22 | 50.04 | 39.25 | 70.71 | 21.67 | 13.63 | 37.60 |
| LogCL | 48.87 | 37.76 | 70.26 | 35.67 | 24.53 | 57.74 | 57.04 | 46.07 | 77.87 | 23.75 | 14.64 | 42.33 |
| DyMemR | 46.12 | 36.38 | 65.15 | 35.50 | 25.29 | 55.44 | 53.76 | 44.68 | 70.84 | 25.46 | 16.79 | 42.49 |
| HisRES | <u>50.48</u> | <u>39.57</u> | <u>71.09</u> | <u>37.69</u> | <u>26.46</u> | <u>59.70</u> | <u>59.07</u> | <u>48.62</u> | <u>78.48</u> | <u>26.58</u> | <u>16.90</u> | <u>46.31</u> |
| CHE-TKG | 51.91 | 41.37 | 72.17 | 38.77 | 27.58 | 60.95 | 60.37 | 50.04 | 79.44 | 27.38 | 17.73 | 47.02 |

Theorem 1 (Ranking Error Reduction). *Let γ_D and γ_E denote the pairwise ranking margins induced by the evolutionary dynamics view and the historical evidence view, respectively. Under the Gaussian margin model above, if the two view-specific margins satisfy $\mathbb{E}[\gamma_D] > 0$, $\mathbb{E}[\gamma_E] > 0$, and $\text{Corr}(\gamma_D, \gamma_E) = \rho < 1$, then the fused margin $\gamma_{D+E} = \gamma_D + \gamma_E$ satisfies*

$$P(\gamma_{D+E} \leq 0) < P(\gamma_D \leq 0) = P(\gamma_E \leq 0). \quad (14)$$

The first condition in Theorem 1, namely $\mathbb{E}[\gamma_D] > 0$ and $\mathbb{E}[\gamma_E] > 0$, characterizes the **View Effectiveness** property: each view provides positive ranking signals on average. The second condition, $\text{Corr}(\gamma_D, \gamma_E) = \rho < 1$, characterizes the **View Non-redundancy** property: the ranking signals from the two views are not perfectly redundant. We refer to signals satisfying both properties as **complementary predictive signals**, i.e., effective and non-redundant pairwise ranking margins. CHE-TKG is designed to learn such complementary predictive signals by explicitly separating historical evidence and evolutionary dynamics into two view-specific structural views. Relation decomposition preserves view-specific relation semantics, while contrastive alignment maintains prediction-aligned semantic consistency across views, jointly encouraging the two views to be both effective and non-redundant. Complementary predictive signals are empirically validated in Section 4.5, and the proof of Theorem 1 is provided in Appendix D.

4 Experiments

4.1 Experimental Settings

Datasets. We evaluate our method on four widely used benchmark datasets for TKG extrapolation: ICEWS14s, ICEWS18, ICEWS05-15, and GDEL T, adopting the standard data splits provided by prior works [30, 31, 9, 54].

Evaluation Protocols. Following prior work, we evaluate the entity extrapolation task using time-aware filtered metrics, including Mean Reciprocal Rank (MRR) and Hits@{1, 10}, and report all results in percentage form. All results are averaged over three runs with different random seeds.

Compared Baselines. We compare our method with a diverse set of embedding-based baselines, including RE-NET [19], RE-GCN [30], RETIA [33], RPC [31], TANGO [17], HisMatch [29], CEN [28], HTCCN [8], HERLN [13], TiRGN [27], LogCL [9], DyMemR [52], and HisRES [54].

More detailed experimental settings and analyses, including ablation study, sensitivity analysis, analysis of complementary predictive signals, statistical analysis of results, relation prediction, robustness analysis, visualization analysis, complexity analysis, and execution time analysis, are provided in Appendix E.

4.2 Main Results

Table 1 reports the time-aware filtered evaluation results for the entity extrapolation task on four benchmark datasets. Overall, CHE-TKG consistently outperforms all the strong baselines. Specifically, relative to the second-best results, CHE-TKG obtains substantial MRR improvements of 2.9%, 3.2%, 2.3%, and 3.1% on ICEWS14s, ICEWS18, ICEWS05-15, and GDELT, respectively. These consistent gains indicate the advantage of our approach, which explicitly separates and jointly models historical evidence and evolutionary dynamics, and further leverages relation decomposition and contrastive alignment to better preserve and exploit complementary predictive signals, thereby improving ranking reliability and prediction accuracy. Overall, the results verify the effectiveness of our CHE-TKG for TKGR.

4.3 Ablation Study

We conduct ablation studies on ICEWS14s and ICEWS18 using MRR and Hits@{1,10}. The results are summarized in Table 2, which reports the following variants: the full CHE-TKG; CHE-TKG without the evolutionary dynamics graph (-w/o- \mathcal{G}^D); without the historical evidence graph (-w/o- \mathcal{G}^E); without both contrastive alignment and relation decomposition, while using both graphs (-w/o-(CoA & ReD)); without contrastive alignment, while using both graphs and relation decomposition (-w/o-CoA); and without disentangled learning (-w/o-DiL).

Overall, removing either the historical evidence graph or the evolutionary dynamics graph results in substantial performance degradation, whereas jointly modeling both consistently yields the best results, validating the effectiveness of the proposed collaborative learning framework. Excluding relation decomposition or contrastive alignment also results in clear performance drops, highlighting the importance of view-specific relation representations and cross-view alignment for suppressing view-specific noise. We further conduct a simple coupled learning variant (-w/o-DiL), where the historical evidence graph is learned first, followed by the evolutionary dynamics graph. This variant surpasses both single-graph counterparts, highlighting the importance of collaborative learning over the two views. However, it still underperforms compared to the variant that jointly learns from both graphs (-w/o-(CoA & ReD)), and further falls short of the full CHE-TKG. This highlights the effectiveness of our approach in better preserving and exploiting complementary predictive signals.

Table 2: Ablation results on ICEWS14s and ICEWS18.

| Variant | ICEWS14s | | | ICEWS18 | | |
|-----------------------|--------------|--------------|--------------|--------------|--------------|--------------|
| | MRR | Hits@1 | Hits@10 | MRR | Hits@1 | Hits@10 |
| CHE-TKG | 51.91 | 41.37 | 72.17 | 38.77 | 27.58 | 60.95 |
| -w/o- \mathcal{G}^D | 49.54 | 38.82 | 70.00 | 36.88 | 25.53 | 59.40 |
| -w/o- \mathcal{G}^E | 50.29 | 39.75 | 70.55 | 36.98 | 25.81 | 58.92 |
| -w/o-(CoA & ReD) | 51.37 | 40.91 | 71.50 | 38.42 | 27.15 | 60.80 |
| -w/o-CoA | 51.70 | 41.19 | 71.73 | 38.62 | 27.46 | 60.57 |
| -w/o-DiL | 51.03 | 40.41 | 71.13 | 38.13 | 26.73 | 60.56 |

4.4 Case Study

To further demonstrate the effectiveness of CHE-TKG, we conduct a qualitative analysis on two representative facts from the ICEWS14s dataset using different model variants. The results are reported in Table 3, where “CHE-TKG-w/ \mathcal{G}^D ” and “CHE-TKG-w/ \mathcal{G}^E ” denote variants that rely solely on the evolutionary dynamics graph and the historical evidence graph, respectively, and “CHE-TKG” represents the full model. The ground-truth entity for each query is highlighted in bold, and the top-ranked entities under the Hits@5 setting along with their scores are reported. From the first example, the ground-truth entity *Employee (India)* appears in the top-5 predictions when using either graph alone, but is not ranked at the top by either variant. By combining scores from both graph views, CHE-TKG assigns the highest score to the ground-truth entity, leading to a correct prediction. These cases demonstrate that the historical evidence graph and the evolutionary dynamics graph provide non-redundant information. Similar observations can be made for the other example.

Table 3: Case study of CHE-TKG’s entity extrapolation performance on the ICEWS14s dataset. The ground-truth entity is highlighted in bold, and the corresponding prediction scores are provided.

| Query | CHE-TKG-w/ \mathcal{G}^D | | CHE-TKG-w/ \mathcal{G}^E | | CHE-TKG | |
|---|-------------------------------------|---------------|--|---------------|-------------------------------------|----------------|
| | Hits@5 Entity | Score | Hits@5 Entity | Score | Hits@5 Entity | Score |
| e_s : Head_of _Government_(India) r : Praise_or_endorse t : 2014 - 12 - 01 | <i>Member_of_Parliament_(India)</i> | 5.1521 | <i>Citizen_(India)</i> | 4.6465 | Employee_(India) | 9.5145 |
| | <i>Governor_(India)</i> | 5.1514 | <i>Company_-_Owner_or_Operator_(India)</i> | 4.4339 | <i>Member_of_Parliament_(India)</i> | 9.1098 |
| | Employee_(India) | 5.1435 | <i>Indigenous_People_(India)</i> | 4.4003 | <i>Governor_(India)</i> | 8.9817 |
| | <i>Labor_Union_(India)</i> | 4.4350 | Employee_(India) | 4.3710 | <i>Citizen_(India)</i> | 8.7354 |
| | <i>Administrative_Body_(India)</i> | 4.3371 | <i>Villager_(India)</i> | 4.2844 | <i>Labor_Union_(India)</i> | 7.9872 |
| e_s : Afghanistan r : Engage_in_negotiation t : 2014 - 12 - 25 | <i>Abdullah_Abdullah</i> | 8.0501 | <i>Iraq</i> | 10.2351 | Tajikistan | 16.7835 |
| | <i>Raheel_Sharif</i> | 8.0464 | Tajikistan | 9.9402 | <i>Iraq</i> | 15.1064 |
| | <i>China</i> | 7.3678 | <i>Afghanistan</i> | 9.1128 | <i>China</i> | 14.8508 |
| | <i>Refugee_(Afghanistan)</i> | 7.0583 | <i>Iran</i> | 7.9106 | <i>Iran</i> | 14.1855 |
| | Tajikistan | 6.8432 | <i>China</i> | 7.4830 | <i>Afghanistan</i> | 12.9165 |

Jointly modeling both views enables more accurate and reliable entity extrapolation, highlighting the effectiveness of the proposed collaborative learning framework.

4.5 Analysis of Complementary Predictive Signals

We compute pair-level score margins and report the statistics in Table 4. As shown in the table, across all datasets, both $\tilde{\gamma}_D$ and $\tilde{\gamma}_E$ are positive, and the pairwise correlation ρ_{pair} is smaller than 1. These observations empirically validate the existence of complementary predictive signals as characterized in Theorem 1. Although the empirical margins do not exactly satisfy the identical-marginal assumption, the observed trend is consistent with the theorem. We further report the pairwise error probabilities P_{err}^D , P_{err}^E , and P_{err}^{D+E} . The results show that $P_{\text{err}}^{D+E} < \min\{P_{\text{err}}^D, P_{\text{err}}^E\}$, which is consistent with the theoretical results in Theorem 1. This reduction in pairwise ranking errors also provides an explanation for the improvement in MRR and Hits@K. For each query, the rank of the ground-truth entity is determined by the number of negative entities that receive higher scores. Therefore, reducing the probability that negative entities outrank the ground-truth entity improves ranking reliability and leads to better MRR and Hits@K.

Table 4: Statistics on different datasets.

| Dataset | $\tilde{\gamma}_D$ | $\tilde{\gamma}_E$ | $\tilde{\gamma}_{D+E}$ | ρ_{pair} | P_{err}^D | P_{err}^E | P_{err}^{D+E} |
|------------|--------------------|--------------------|------------------------|----------------------|--------------------|--------------------|------------------------|
| ICEWS14s | 7.17 | 5.78 | 12.95 | 0.723 | 0.0206 | 0.0283 | 0.0196 |
| ICEWS18 | 7.45 | 5.45 | 12.90 | 0.754 | 0.0151 | 0.0186 | 0.0141 |
| ICEWS05-15 | 8.51 | 5.24 | 13.75 | 0.724 | 0.0187 | 0.0280 | 0.0178 |
| GDELT | 6.28 | 3.89 | 10.17 | 0.750 | 0.0163 | 0.0203 | 0.0139 |

5 Conclusion

In this work, we proposed CHE-TKG, a collaborative dual-view learning framework for TKGR. CHE-TKG explicitly separates historical evidence and evolutionary dynamics into two view-specific structural views, allowing the model to learn complementary predictive signals for future fact prediction. The historical evidence view captures long-term structural regularities, while the evolutionary dynamics view models temporal transitions and recent changes. Relation decomposition and contrastive alignment are further introduced to learn view-specific relation semantics and promote task-relevant complementarity between the two views. We provided a theoretical analysis showing that effective and non-redundant predictive signals can improve ranking reliability by reducing pair-level ranking errors. Experiments on multiple benchmark datasets demonstrate that CHE-TKG achieves state-of-the-art performance in extrapolation settings. Overall, these results highlight the benefits of collaboratively modeling historical evidence and evolutionary dynamics for TKGR.

References

- [1] Farah Atif, Ola El Khatib, and Djellel Difallah. Beamqa: Multi-hop knowledge graph question answering with sequence-to-sequence prediction and beam search. In *Proceedings of the ACM SIGIR Conference on Research and Development in Information Retrieval*, pages 781–790, 2023.
- [2] Long Bai, Zixuan Li, Xiaolong Jin, Jiafeng Guo, Xueqi Cheng, and Tat-Seng Chua. G2s: A general-to-specific learning framework for temporal knowledge graph forecasting with large language models. *Findings of the Association for Computational Linguistics: ACL*, 2025.
- [3] Antoine Bordes, Nicolas Usunier, Alberto Garcia-Duran, Jason Weston, and Oksana Yakhnenko. Translating embeddings for modeling multi-relational data. *Advances in neural information processing systems*, 2013.
- [4] Elizabeth Boschee, Jennifer Lautenschlager, Sean O’Brien, Steve Shellman, James Starz, and Michael Ward. ICEWS Coded Event Data, 2015.
- [5] Ling Chen, Xing Tang, Weiqi Chen, Yuntao Qian, Yansheng Li, and Yongjun Zhang. Dacha: A dual graph convolution based temporal knowledge graph representation learning method using historical relation. *ACM Transactions on Knowledge Discovery from Data*, pages 1–18, 2021.
- [6] Qian Chen and Ling Chen. Decrl: A deep evolutionary clustering jointed temporal knowledge graph representation learning approach. *Advances in Neural Information Processing Systems*, 37:55204–55227, 2024.
- [7] Qian Chen, Jinyu Zhang, and Ling Chen. Beyond entity correlations: Disentangling event causal puzzles in temporal knowledge graphs. In *International Conference on Learning Representations*, 2026.
- [8] Tingxuan Chen, Jun Long, Liu Yang, Zidong Wang, Yongheng Wang, and Xiongnan Jin. Htcn: Temporal causal convolutional networks with hawkes process for extrapolation reasoning in temporal knowledge graphs. In *Proceedings of the North American Chapter of the Association for Computational Linguistics*, pages 4056–4066, 2024.
- [9] Wei Chen, Huaiyu Wan, Yuting Wu, Shuyuan Zhao, Jiayaqi Cheng, Yuxin Li, and Youfang Lin. Local-global history-aware contrastive learning for temporal knowledge graph reasoning. In *IEEE International Conference on Data Engineering (ICDE)*, pages 733–746. IEEE, 2024.
- [10] Songgaojun Deng, Huzefa Rangwala, and Yue Ning. Dynamic knowledge graph based multi-event forecasting. In *Proceedings of the 26th ACM SIGKDD international conference on knowledge discovery & data mining*, pages 1585–1595, 2020.
- [11] Wentao Ding, Jinmao Li, Liangchuan Luo, and Yuzhong Qu. Enhancing complex question answering over knowledge graphs through evidence pattern retrieval. In *Proceedings of the ACM Web Conference*, pages 2106–2115, 2024.
- [12] Hao Dong, Zhiyuan Ning, Pengyang Wang, Ziyue Qiao, Pengfei Wang, Yuanchun Zhou, and Yanjie Fu. Adaptive path-memory network for temporal knowledge graph reasoning. In *Proceedings of the International Joint Conference on Artificial Intelligence*, pages 2086–2094, 2023.
- [13] Yuwei Du, Xinyue Liu, Wenxin Liang, Linlin Zong, and Xianchao Zhang. Hawkes based representation learning for reasoning over scale-free community-structured temporal knowledge graphs. In *Proceedings of the International Conference on Computational Linguistics*, pages 2935–2946, 2025.
- [14] Zhiyu Fang, Shuai-Long Lei, Xiaobin Zhu, Chun Yang, Shi-Xue Zhang, Xu-Cheng Yin, and Jingyan Qin. Transformer-based reasoning for learning evolutionary chain of events on temporal knowledge graph. In *Proceedings of the ACM SIGIR Conference on Research and Development in Information Retrieval*, pages 70–79, 2024.

- [15] Zhiyu Fang, Jingyan Qin, Xiaobin Zhu, Chun Yang, and Xu-Cheng Yin. Arbitrary time information modeling via polynomial approximation for temporal knowledge graph embedding. In *Proceedings of the Joint International Conference on Computational Linguistics, Language Resources and Evaluation*, pages 1455–1465, 2024.
- [16] Julia Gastinger, Timo Sztyler, Lokesh Sharma, and Anett Schuelke. On the evaluation of methods for temporal knowledge graph forecasting. In *NeurIPS Temporal Graph Learning Workshop*, 2022.
- [17] Zhen Han, Zifeng Ding, Yunpu Ma, Yujia Gu, and Volker Tresp. Learning neural ordinary equations for forecasting future links on temporal knowledge graphs. In *Proceedings of the Conference on Empirical Methods in Natural Language Processing*, pages 8352–8364, 2021.
- [18] Rikui Huang, Wei Wei, Xiaoye Qu, Shengzhe Zhang, Dangyang Chen, and Yu Cheng. Confidence is not timeless: Modeling temporal validity for rule-based temporal knowledge graph forecasting. In *Proceedings of the Annual Meeting of the Association for Computational Linguistics*, pages 10783–10794, 2024.
- [19] Woojeong Jin, Meng Qu, Xisen Jin, and Xiang Ren. Recurrent event network: Autoregressive structure inference over temporal knowledge graphs. In *Proceedings of the 2020 conference on empirical methods in natural language processing (EMNLP)*, pages 6669–6683, 2020.
- [20] Timothée Lacroix, Guillaume Obozinski, and Nicolas Usunier. Tensor decompositions for temporal knowledge base completion. In *International Conference on Learning Representations*, 2020.
- [21] Julien Leblay and Melisachew Wudage Chekol. Deriving validity time in knowledge graph. In *Proceedings of the ACM Web Conference*, 2018.
- [22] Dong-Ho Lee, Kian Ahrabian, Woojeong Jin, Fred Morstatter, and Jay Pujara. Temporal knowledge graph forecasting without knowledge using in-context learning. In *Proceedings of the Conference on Empirical Methods in Natural Language Processing*, pages 544–557, 2023.
- [23] Kalev Leetaru and Philip A Schrod. Gdelt: Global data on events, location, and tone. In *ISA Annual Convention*, pages 1–49, 2013.
- [24] Jiang Li, Xiangdong Su, and Guanglai Gao. Teast: Temporal knowledge graph embedding via archimedean spiral timeline. In *Proceedings of the Annual Meeting of the Association for Computational Linguistics*, pages 15460–15474, 2023.
- [25] Ningyuan Li, E Haihong, Shi Li, Mingzhi Sun, Tianyu Yao, Meina Song, Yong Wang, and Haoran Luo. Tr-rules: Rule-based model for link forecasting on temporal knowledge graph considering temporal redundancy. In *Findings of the Association for Computational Linguistics: EMNLP*, pages 7885–7894, 2023.
- [26] Ningyuan Li, E Haihong, Tianyu Yao, Tianyi Hu, Yuhan Li, Haoran Luo, Meina Song, and Yifan Zhu. Infer: A neural-symbolic model for extrapolation reasoning on temporal knowledge graph. In *International Conference on Learning Representations*, 2025.
- [27] Yujia Li, Shiliang Sun, and Jing Zhao. Tirgn: Time-guided recurrent graph network with local-global historical patterns for temporal knowledge graph reasoning. In *Proceedings of the International Joint Conference on Artificial Intelligence*, pages 2152–2158, 2022.
- [28] Zixuan Li, Saiping Guan, Xiaolong Jin, Weihua Peng, Yajuan Lyu, Yong Zhu, Long Bai, Wei Li, Jiafeng Guo, and Xueqi Cheng. Complex evolutionary pattern learning for temporal knowledge graph reasoning. In *Proceedings of the Annual Meeting of the Association for Computational Linguistics*, pages 290–296, 2022.
- [29] Zixuan Li, Zhongni Hou, Saiping Guan, Xiaolong Jin, Weihua Peng, Long Bai, Yajuan Lyu, Wei Li, Jiafeng Guo, and Xueqi Cheng. Hismatch: Historical structure matching based temporal knowledge graph reasoning. In *Findings of the Association for Computational Linguistics: EMNLP*, pages 7328–7338, 2022.

- [30] Zixuan Li, Xiaolong Jin, Wei Li, Saiping Guan, Jiafeng Guo, Huawei Shen, Yuanzhuo Wang, and Xueqi Cheng. Temporal knowledge graph reasoning based on evolutionary representation learning. In *Proceedings of the ACM SIGIR Conference on Research and Development in Information Retrieval*, pages 408–417, 2021.
- [31] Ke Liang, Lingyuan Meng, Meng Liu, Yue Liu, Wenxuan Tu, Siwei Wang, Sihang Zhou, and Xinwang Liu. Learn from relational correlations and periodic events for temporal knowledge graph reasoning. In *Proceedings of the ACM SIGIR Conference on Research and Development in Information Retrieval*, pages 1559–1568, 2023.
- [32] Ruotong Liao, Xu Jia, Yangzhe Li, Yunpu Ma, and Volker Tresp. Gentkg: Generative forecasting on temporal knowledge graph with large language models. In *Findings of the Association for Computational Linguistics: NAACL*, pages 4303–4317, 2024.
- [33] Kangzheng Liu, Feng Zhao, Guandong Xu, Xianzhi Wang, and Hai Jin. Retia: relation-entity twin-interact aggregation for temporal knowledge graph extrapolation. In *IEEE International Conference on Data Engineering (ICDE)*, pages 1761–1774. IEEE, 2023.
- [34] Lihui Liu, Boxin Du, Jiejun Xu, Yinglong Xia, and Hanghang Tong. Joint knowledge graph completion and question answering. In *Proceedings of the ACM SIGKDD International Conference on Knowledge Discovery & Data Mining*, pages 1098–1108, 2022.
- [35] Yushan Liu, Yunpu Ma, Marcel Hildebrandt, Mitchell Joblin, and Volker Tresp. Tlogic: Temporal logical rules for explainable link forecasting on temporal knowledge graphs. In *Proceedings of the AAAI Conference on Artificial Intelligence*, pages 4120–4127, 2022.
- [36] Ziyang Liu and Chaokun Wang. Terdy: Temporal relation dynamics through frequency decomposition for temporal knowledge graph completion. In *Proceedings of the Annual Meeting of the Association for Computational Linguistics*, pages 9611–9622, 2025.
- [37] Johannes Messner, Ralph Abboud, and Ismail Ilkan Ceylan. Temporal knowledge graph completion using box embeddings. In *Proceedings of the AAAI Conference on Artificial Intelligence*, pages 7779–7787, 2022.
- [38] Mohammad Pezeshki, Oumar Kaba, Yoshua Bengio, Aaron C Courville, Doina Precup, and Guillaume Lajoie. Gradient starvation: A learning proclivity in neural networks. In *Advances in Neural Information Processing Systems*, pages 1256–1272, 2021.
- [39] Luca Scimeca, Seong Joon Oh, Sanghyuk Chun, Michael Poli, and Sangdoon Yun. Which shortcut cues will dnns choose? a study from the parameter-space perspective. In *International Conference on Learning Representations*, 2022.
- [40] Noam Shazeer. Glu variants improve transformer. *arXiv preprint arXiv:2002.05202*, 2020.
- [41] Haohai Sun, Shangyi Geng, Jialun Zhong, Han Hu, and Kun He. Graph hawkes transformer for extrapolated reasoning on temporal knowledge graphs. In *Proceedings of the Conference on Empirical Methods in Natural Language Processing*, pages 7481–7493, 2022.
- [42] Gu Tang, Xiaoying Gan, Jinghe Wang, Bin Lu, Lyuwen Wu, Luoyi Fu, and Chenghu Zhou. Editkg: Editing knowledge graph for recommendation. In *Proceedings of the ACM SIGIR Conference on Research and Development in Information Retrieval*, pages 112–122, 2024.
- [43] Guo Tang, Zheng Chu, Wenxiang Zheng, Junjia Xiang, Yizhuo Li, Weihao Zhang, Ming Liu, and Bing Qin. Anre: Analogical replay for temporal knowledge graph forecasting. In *Proceedings of the Annual Meeting of the Association for Computational Linguistics*, pages 4632–4650, 2025.
- [44] Xing Tang and Ling Chen. Gtrl: An entity group-aware temporal knowledge graph representation learning method. *IEEE Transactions on Knowledge and Data Engineering*, 36(9):4707–4721, 2023.
- [45] Xing Tang, Ling Chen, Hongyu Shi, and Dandan Lyu. Dhyper: A recurrent dual hypergraph neural network for event prediction in temporal knowledge graphs. *ACM Transactions on Information Systems*, 42(5):1–23, 2024.

- [46] Jiapu Wang, Kai Sun, Linhao Luo, Wei Wei, Yongli Hu, Alan W Liew, Shirui Pan, and Baocai Yin. Large language models-guided dynamic adaptation for temporal knowledge graph reasoning. *Advances in Neural Information Processing Systems*, pages 8384–8410, 2024.
- [47] Jihu Wang, Yuliang Shi, Han Yu, Xinjun Wang, Zhongmin Yan, and Fanyu Kong. Mixed-curvature manifolds interaction learning for knowledge graph-aware recommendation. In *Proceedings of the ACM SIGIR Conference on Research and Development in Information Retrieval*, pages 372–382, 2023.
- [48] Yuwei Xia, Ding Wang, Qiang Liu, Liang Wang, Shu Wu, and Xiao-Yu Zhang. Chain-of-history reasoning for temporal knowledge graph forecasting. In *Findings of the Association for Computational Linguistics: ACL*, pages 16144–16159, 2024.
- [49] Da Xu, Chuanwei Ruan, Evren Korpeoglu, Sushant Kumar, and Kannan Achan. Inductive representation learning on temporal graphs. In *International Conference on Learning Representations*, 2020.
- [50] Zhentao Xu, Mark Jerome Cruz, Matthew Guevara, Tie Wang, Manasi Deshpande, Xiaofeng Wang, and Zheng Li. Retrieval-augmented generation with knowledge graphs for customer service question answering. In *Proceedings of the ACM SIGIR Conference on Research and Development in Information Retrieval*, pages 2905–2909, 2024.
- [51] Rui Ying, Mengting Hu, Jianfeng Wu, Yalan Xie, Xiaoyi Liu, Zhunheng Wang, Ming Jiang, Hang Gao, Linlin Zhang, and Renhong Cheng. Simple but effective compound geometric operations for temporal knowledge graph completion. In *Proceedings of the Annual Meeting of the Association for Computational Linguistics*, pages 11074–11086, 2024.
- [52] Fuwei Zhang, Zhao Zhang, Fuzhen Zhuang, Yu Zhao, Deqing Wang, and Hongwei Zheng. Temporal knowledge graph reasoning with dynamic memory enhancement. *IEEE Transactions on Knowledge and Data Engineering*, 36(11):7115–7128, 2024.
- [53] Jiasheng Zhang, Shuang Liang, Yongpan Sheng, and Jie Shao. Temporal knowledge graph representation learning with local and global evolutions. *Knowledge-Based Systems*, 251:109234, 2022.
- [54] Jinchuan Zhang, Ming Sun, Chong Mu, Jinhao Zhang, Quanjiang Guo, and Ling Tian. Historically relevant event structuring for temporal knowledge graph reasoning. In *IEEE International Conference on Data Engineering (ICDE)*, pages 3179–3192. IEEE, 2025.
- [55] Mengqi Zhang, Yuwei Xia, Qiang Liu, Shu Wu, and Liang Wang. Learning latent relations for temporal knowledge graph reasoning. In *Proceedings of the Annual Meeting of the Association for Computational Linguistics*, pages 12617–12631, 2023.
- [56] Mengqi Zhang, Yuwei Xia, Qiang Liu, Shu Wu, and Liang Wang. Learning long-and short-term representations for temporal knowledge graph reasoning. In *Proceedings of the ACM Web Conference*, pages 2412–2422, 2023.

A Related Work

A.1 Differences from Local-Based Methods

Our method differs fundamentally from prior approaches such as HGLS [56], LogCL [9], and HisRES [54]. These methods typically exploit recent snapshots as local information, which is substantially different from the evolutionary dynamics modeled in our framework. It is important to distinguish local-based modeling from evolutionary dynamics. Local-based modeling captures temporal context from recent snapshots, often via GNNs and recurrent modules, and serves as a general-purpose representation learning component. In contrast, evolutionary dynamics are modeled from a predictive perspective, focusing on task-relevant temporal transitions of entities and relations. Moreover, evolutionary dynamics capture logically related events across multiple timestamps, resulting in substantially broader temporal coverage than local-based modeling. In other words, local-based modeling provides general contextual information, whereas evolutionary dynamics capture predictive signals. They differ fundamentally in their role, modeling level, and objective.

Table 5: Performance of TKG entity extrapolation on ICEWS14s, ICEWS18, and ICEWS05-15. The time-aware filtered MRR, Hits@1, and Hits@10 metrics are multiplied by 100. The best results are marked in **bold**.

| Type | Model | ICEWS14s | | | ICEWS18 | | | ICEWS05-15 | | |
|------------|-----------|--------------|--------------|--------------|--------------|--------------|--------------|--------------|--------------|--------------|
| | | MRR | Hits@1 | Hits@10 | MRR | Hits@1 | Hits@10 | MRR | Hits@1 | Hits@10 |
| Path-based | TLogic | 43.04 | 33.56 | 61.23 | 29.82 | 20.54 | 48.53 | 46.97 | 36.21 | 67.43 |
| | TR-Rules | 43.32 | 33.96 | 61.17 | 30.41 | 21.10 | 48.92 | 47.64 | 37.06 | 67.57 |
| | TempValid | 45.78 | 35.50 | 65.06 | 33.50 | 23.91 | 52.33 | 50.31 | 39.46 | 70.55 |
| | INFER | 44.46 | 35.03 | 62.31 | 32.22 | 22.39 | 51.52 | 48.73 | 38.32 | 68.48 |
| LLM-based | GenTKG | – | 36.85 | 53.50 | – | 24.25 | 42.10 | – | – | – |
| | LLM-DA | 47.10 | 36.90 | 67.10 | – | – | – | 52.10 | 41.60 | 72.80 |
| | MESH | 44.36 | – | 64.21 | 33.96 | – | 54.12 | 48.66 | – | 68.57 |
| | AnRe | 47.40 | 36.90 | 65.70 | 35.50 | 26.00 | 56.70 | 50.90 | 39.10 | 69.60 |
| Dual-views | CHE-TKG | 51.91 | 41.37 | 72.17 | 38.77 | 27.58 | 60.95 | 60.37 | 50.04 | 79.44 |

A.2 Interpolation Reasoning

Interpolation reasoning focuses on inferring facts at observed past timestamps. Many existing methods aim to capture temporal dependencies through diverse modeling strategies [21, 20, 37, 14, 15, 36, 51, 24]. For example, TTransE [21] extends TransE [3] by modeling time and relations as translation operations, while TComplex [20] captures temporal dependencies while supporting atemporal facts. BoxTE [37] incorporates temporal information via relation-specific transition matrices, and ECEformer [14] models temporal patterns through evolutionary event chains. Recently, several approaches have explored modeling TKGs in the complex-valued space. TCompoundE [51] models temporal KGs via relation- and time-specific translation and scaling transformations. TeRDy [36] decomposes relation embeddings in the frequency domain to capture long- and short-term dynamics.

A.3 Extrapolation Reasoning

Beyond embedding-based methods, extrapolation approaches can also be categorized into rule-based and LLM-based methods.

Rule-Based TKGR. TLogic [35] extracts temporal logical rules via non-increasing temporal random walks, estimates rule confidence, and derives predictions through noisy-OR aggregation. Subsequent methods extend this framework. TR-Rules [25] mines temporal acyclic rules and introduces window-based confidence to mitigate temporal redundancy, while TempValid [18] further incorporates temporal decay into rule confidence estimation. Unlike TLogic and its variants, INFER [26] incorporates temporal validity, fact frequency, and embedding information for extrapolation reasoning, while DaeMon [12] learns continuous and implicit path representations through neural networks without explicitly constructing logical rules.

LLM-Based TKGR. Recently, several studies explore leveraging the inductive and reasoning capabilities of large language models (LLMs) for TKGR. ICL [22] applies in-context learning by prompting LLMs with historical inputs, while GenTKG [32] and LLM-DA [46] incorporate temporal logical rules to retrieve and refine historical sequences. CoH [48] leverages LLMs to explore high-order historical chains and combines their semantic reasoning with structural predictions from graph models. G2S [2] adopts a two-stage framework that combines ID-based quadruples with textual representations, and AnRe [43] further enhances temporal reasoning by guiding LLMs with few-shot analogical examples.

We further compare our method with rule-based and LLM-based approaches. As shown in Table 5 on ICEWS14s, ICEWS18, and ICEWS05-15, our method still achieves the best performance. It is worth noting that most of these methods are evaluated on these datasets instead of GDEL, likely due to the substantially larger scale of GDEL.

B List of Notations

We summarize the main notations used in this paper in Table 6.

Table 6: Summary of Important Notations

| Notation | Description |
|--|--|
| $\mathcal{E}, \mathcal{R}, \mathcal{T}, \mathcal{F}$ | Entity, relation, timestamp, and temporal fact set in a TKG. |
| \mathcal{G}_t | Temporal knowledge graph snapshot at timestamp t . |
| $\mathbf{e}_{s,t}, \mathbf{r}_t, \mathbf{e}_{o,t}$ | Subject, relation, and object embeddings at timestamp t . |
| $\mathbf{E}_t, \mathbf{R}_t$ | Entity and relation embedding matrices at timestamp t . |
| $\mathcal{G}^D, \mathcal{G}^E$ | Evolutionary dynamics and historical evidence graph. |
| $\mathbf{e}^D, \mathbf{e}^E$ | Entity embeddings of both graphs. |
| $\mathbf{r}^D, \mathbf{r}^E$ | Relation embeddings of both graphs. |
| $\mathbf{E}^D, \mathbf{E}^E$ | Entity embedding matrices of both graphs. |
| $\mathbf{R}^D, \mathbf{R}^E$ | Relation embedding matrices of both graphs. |
| d | Embedding dimensionality. |
| L | Number of historical snapshots used for modeling. |
| \mathcal{Q}_{t_q} | Set of prediction queries associated with timestamp t_q . |

C Analysis of Rule-Based Retrieval

In this section, we analyze temporal logical rule-based retrieval used to construct the evolutionary dynamics graph. The rules are learned using the standard TLogic [35] procedure, relying solely on training data. In practice, we restrict rule retrieval to one-hop rules for efficiency and reliability, and skip rule-based retrieval for relations that are not covered by any mined rule. We report the learned rules on the ICEWS14s, ICEWS18, ICEWS05-15, and GDELT datasets, along with the coverage of retrieved evolutionary dynamics facts on the test set, as shown in Table 7.

Rule-Cov. denotes the fraction of test queries whose query relation is covered by at least one mined temporal rule. **Retrieved-Cov.** denotes the fraction of test queries for which the mined rules retrieve at least one historical fact. **Avg. Retrieved Facts** denotes the average number of retrieved facts per query. As shown in the table, the majority of test queries are associated with at least one retrieved evolutionary dynamics fact. For queries with zero retrieved facts, the model cannot rely on explicit evolutionary dynamics and instead makes predictions based on latent entity and relation representations. Furthermore, restricting to one-hop rules still allows the model to effectively capture temporal evolution patterns of entities.

Table 7: Statistics of rule-based retrieval on different datasets.

| Dataset | Rule-Cov. | Retrieved-Cov. | Avg. Retrieved Facts |
|------------|-----------|----------------|----------------------|
| ICEWS14s | 100.00 | 95.849 | 8.7331 |
| ICEWS18 | 99.976 | 97.321 | 7.4332 |
| ICEWS05-15 | 99.985 | 98.911 | 9.5729 |
| GDELT | 99.999 | 99.780 | 7.9673 |

D Proofs

In this section, we provide a proof of Theorem 1.

Proof. Assume (γ_D, γ_E) follows a joint Gaussian distribution with identical marginals:

$$\gamma_D, \gamma_E \sim \mathcal{N}(\mu, \sigma^2), \quad (15)$$

and correlation coefficient

$$\text{Corr}(\gamma_D, \gamma_E) = \rho < 1. \quad (16)$$

Define the fused margin:

$$\gamma_{D+E} = \gamma_D + \gamma_E. \quad (17)$$

Since a linear combination of jointly Gaussian variables remains Gaussian, we have

$$\gamma_{D+E} \sim \mathcal{N}(\mathbb{E}[\gamma_{D+E}], \text{Var}(\gamma_{D+E})). \quad (18)$$

The expectation is

$$\mathbb{E}[\gamma_{D+E}] = \mathbb{E}[\gamma_D] + \mathbb{E}[\gamma_E] = 2\mu. \quad (19)$$

The variance is

$$\text{Var}(\gamma_{D+E}) = \text{Var}(\gamma_D) + \text{Var}(\gamma_E) + 2 \text{Cov}(\gamma_D, \gamma_E). \quad (20)$$

Using $\text{Var}(\gamma_D) = \text{Var}(\gamma_E) = \sigma^2$ and

$$\text{Cov}(\gamma_D, \gamma_E) = \rho\sigma^2, \quad (21)$$

we obtain

$$\text{Var}(\gamma_{D+E}) = 2\sigma^2(1 + \rho). \quad (22)$$

Thus,

$$\gamma_{D+E} \sim \mathcal{N}(2\mu, 2\sigma^2(1 + \rho)). \quad (23)$$

For a single view, the error probability is

$$P(\gamma_D \leq 0) = P\left(\frac{\gamma_D - \mu}{\sigma} \leq -\frac{\mu}{\sigma}\right) = \Phi\left(-\frac{\mu}{\sigma}\right), \quad (24)$$

where $\Phi(\cdot)$ is the standard normal cumulative distribution function (CDF). Similarly,

$$P(\gamma_E \leq 0) = \Phi\left(-\frac{\mu}{\sigma}\right). \quad (25)$$

For the fused margin,

$$P(\gamma_{D+E} \leq 0) = P\left(\frac{\gamma_{D+E} - 2\mu}{\sqrt{2\sigma^2(1 + \rho)}} \leq -\frac{2\mu}{\sqrt{2\sigma^2(1 + \rho)}}\right), \quad (26)$$

which gives

$$P(\gamma_{D+E} \leq 0) = \Phi\left(-\frac{2\mu}{\sqrt{2\sigma^2(1 + \rho)}}\right) = \Phi\left(-\frac{\sqrt{2}\mu}{\sigma\sqrt{1 + \rho}}\right). \quad (27)$$

Since $\rho < 1$, we have $1 + \rho < 2$, which implies

$$\frac{\sqrt{2}\mu}{\sigma\sqrt{1 + \rho}} > \frac{\mu}{\sigma}. \quad (28)$$

Multiplying both sides by -1 reverses the inequality:

$$-\frac{\sqrt{2}\mu}{\sigma\sqrt{1 + \rho}} < -\frac{\mu}{\sigma}. \quad (29)$$

By the monotonicity of Φ , it follows that

$$P(\gamma_{D+E} \leq 0) < P(\gamma_D \leq 0). \quad (30)$$

Since the two views are symmetric, we also have

$$P(\gamma_D \leq 0) = P(\gamma_E \leq 0). \quad (31)$$

Thus,

$$P(\gamma_{D+E} \leq 0) < P(\gamma_D \leq 0) = P(\gamma_E \leq 0). \quad (32)$$

□

Remark 1. Suppose

$$\gamma_D \sim \mathcal{N}(\mu_D, \sigma_D^2), \quad \gamma_E \sim \mathcal{N}(\mu_E, \sigma_E^2), \quad (33)$$

with correlation ρ . Then

$$\gamma_{D+E} = \gamma_D + \gamma_E \sim \mathcal{N}(\mu_D + \mu_E, \sigma_D^2 + \sigma_E^2 + 2\rho\sigma_D\sigma_E). \quad (34)$$

Table 8: Statistics of datasets

| Dataset | Entities $ \mathcal{E} $ | Relations $ \mathcal{R} $ | Training Facts | Validation Facts | Testing Facts | Timestamps $ \mathcal{T} $ | Time granularity |
|------------|--------------------------|---------------------------|----------------|------------------|---------------|----------------------------|------------------|
| ICEWS14s | 7,128 | 230 | 74,845 | 8,514 | 7,371 | 365 | 24 hours |
| ICEWS18 | 23,033 | 256 | 373,018 | 45,995 | 49,545 | 304 | 24 hours |
| ICEWS05-15 | 10,094 | 251 | 368,868 | 46,302 | 46,159 | 4017 | 24 hours |
| GDELT | 7,691 | 240 | 1,734,399 | 238,765 | 305,241 | 2976 | 15 mins |

The corresponding error probabilities are

$$P(\gamma_D \leq 0) = \Phi\left(-\frac{\mu_D}{\sigma_D}\right), \quad P(\gamma_E \leq 0) = \Phi\left(-\frac{\mu_E}{\sigma_E}\right), \quad (35)$$

and

$$P(\gamma_{D+E} \leq 0) = \Phi\left(-\frac{\mu_D + \mu_E}{\sqrt{\sigma_D^2 + \sigma_E^2 + 2\rho\sigma_D\sigma_E}}\right). \quad (36)$$

Define the signal-to-noise ratios as

$$\text{SNR}_D = \frac{\mu_D}{\sigma_D}, \quad \text{SNR}_E = \frac{\mu_E}{\sigma_E}, \quad (37)$$

and

$$\text{SNR}_{D+E} = \frac{\mu_D + \mu_E}{\sqrt{\sigma_D^2 + \sigma_E^2 + 2\rho\sigma_D\sigma_E}}. \quad (38)$$

Since $\Phi(\cdot)$ is monotonically increasing, if

$$\text{SNR}_{D+E} > \max\{\text{SNR}_D, \text{SNR}_E\}, \quad (39)$$

then

$$P(\gamma_{D+E} \leq 0) < P(\gamma_D \leq 0), \quad P(\gamma_{D+E} \leq 0) < P(\gamma_E \leq 0). \quad (40)$$

Thus, in the general Gaussian case, dual-view fusion reduces the ranking error probability when the fused margin achieves a higher signal-to-noise ratio than either single-view margin.

E Extra Experiments

E.1 Experimental Settings

Datasets. We evaluate our method on four widely used benchmark datasets for TKG extrapolation: ICEWS14s, ICEWS18, ICEWS05-15, and GDELT. The first three datasets are derived from the Integrated Crisis Early Warning System (ICEWS) [4], while GDELT is collected from the Global Database of Events, Language, and Tone [23]. Following prior work, all datasets are split chronologically into training, validation, and test sets with proportions of 80%, 10%, and 10%, respectively. Detailed statistics of the datasets are reported in Table 8. Following recent extrapolation-based TKG studies [54, 9, 55], we do not report results on datasets with coarse temporal granularity (e.g., WIKI and YAGO), which are less suitable for modeling fine-grained temporal dynamics.

Evaluation Protocols. Following prior work [30, 9, 54, 16], we evaluate the entity extrapolation task using time-aware filtered metrics, including Mean Reciprocal Rank (MRR) and Hits@{1, 10}, and report all results in percentage form. Higher values of MRR and Hits@k indicate better performance, which can be formulated as:

$$\text{MRR} = \frac{1}{2 * |\text{test}|} \sum_{f=(e_s, r, e_o, \tau) \in \text{test}} \left(\frac{1}{k_{f,o}} + \frac{1}{k_{f,s}} \right), \quad (41)$$

$$\text{Hits}@k = \frac{1}{2 * |\text{test}|} \sum_{f=(e_s, r, e_o, \tau) \in \text{test}} (\mathbb{1}_{k_{f,o} \leq k} + \mathbb{1}_{k_{f,s} \leq k}), \quad (42)$$

where $k_{f,s}$ and $k_{f,o}$ denote the ranking of subject entity e_s and object entity e_o , respectively. $\mathbb{1}_{\text{condition}}$ is 1 if *condition* holds and 0 otherwise.

Compared Baselines.

- **RE-NET** [19] models event sequences in an autoregressive manner, using RNNs to encode historical events and neighbor aggregation to capture structural information.
- **RE-GCN** [30] employs relation-aware GCNs to model structural dependencies at each timestamp, combined with recurrent units for temporal evolution.
- **RETIA** [33] constructs dual hyper-relational subgraphs to jointly aggregate entity and relation information with bidirectional interactions.
- **RPC** [31] models relational correlations and captures temporal periodic patterns via relation and periodic correspondence modules.
- **TANGO** [17] models continuous-time dynamics using neural ODEs with relational graph convolutions.
- **HiSMATCH** [29] adopts a dual-encoder framework to match query-related and candidate-related historical structures.
- **CEN** [28] captures evolutionary patterns of different lengths via CNNs with curriculum learning.
- **HTCCN** [8] combines causal convolutions with Hawkes processes to model temporal dependencies and event intensities.
- **HERLN** [13] integrates Hawkes processes with structural properties such as community and long-tail distributions.
- **TiRGN** [27] jointly models local temporal dependencies, global historical patterns, and periodicity via hybrid encoders.
- **LogCL** [9] leverages contrastive learning to integrate local and global historical information with query-aware attention.
- **DyMemR** [52] employs a dynamic memory module to store and retrieve important historical facts.
- **HisRES** [54] models multi-granularity temporal interactions and selectively aggregates query-relevant historical information.

Results for HGLS and L²TKG are omitted due to differences in experimental settings. All baseline results are taken from prior work and are reported on the same datasets and under the same filtering protocol for fair comparison. Specifically, the results of RE-NET, RE-GCN, RETIA, RPC, CEN, TiRGN, LogCL and HisRES are taken from HisRES [54]. The result of TANGO is taken from LogCL [9]. The results of HisMatch, HTCCN, HERLN, and DyMemR are taken from their original papers.

Implementation Settings. All experiments are conducted on an NVIDIA RTX P40 GPU. The embedding dimension is set to 200, with a dropout rate of 0.2 for all layers. Models are trained for up to 50 epochs using early stopping based on validation MRR. We use the Adam optimizer with a learning rate of 0.001 and a weight decay of 1×10^{-5} . The historical length in the spatio-temporal initialization module is fixed to 3. The GNN encoder consists of two layers. The relation prediction coefficient α is set to 0.7. Hyperparameters, including the contrastive alignment weight μ , temperature γ , number of GAT layers, and rule graph length, are tuned via grid search on the validation set. For ICEWS14s, ICEWS18, ICEWS05-15, and GDELTA, μ is set to 0.2, 0.01, 0.15, and 0.3, γ to 0.3, 0.03, 0.2, and 0.25, the number of GAT layers to 3, 2, 2, and 2, and the rule graph length to 10, 8, 10, and 8, respectively. Following prior work [30, 27, 31, 9, 54], static KG information is integrated into the ICEWS datasets. We further apply a two-phase forward propagation process to both graph encoders [9, 54], handling raw and inverse query sets separately. As a result, historical evidence graphs and evolutionary dynamics graphs are constructed independently for each query type, preventing potential data leakage.

E.2 Ablation Study

In this subsection, we conduct additional ablation studies to further validate the effectiveness of our design. The results are summarized in Table 9, which reports multiple variants: the full CHE-TKG; without both contrastive alignment and relation decomposition while retaining both graphs (-w/o-(CoA & ReD)); without the historical evidence graph (-w/o- \mathcal{G}^E); replacing the rule-based retrieval strategy with a simple heuristic for constructing \mathcal{G}^D (-w/Simp); introducing entity decomposition

Table 9: Ablation results on ICEWS14s and ICEWS18.

| Variant | ICEWS14s | | | ICEWS18 | | |
|-----------------------|--------------|--------------|--------------|--------------|--------------|--------------|
| | MRR | Hits@1 | Hits@10 | MRR | Hits@1 | Hits@10 |
| CHE-TKG | 51.91 | 41.37 | 72.17 | 38.77 | 27.58 | 60.95 |
| -w/o-(CoA & ReD) | 51.37 | 40.91 | 71.50 | 38.42 | 27.15 | 60.80 |
| -w/o- \mathcal{G}^E | 50.29 | 39.75 | 70.55 | 36.98 | 25.81 | 58.92 |
| -w/Simp | 44.91 | 34.17 | 66.32 | 33.82 | 23.05 | 55.10 |
| -w/EnD | 51.76 | 41.24 | 71.62 | 38.39 | 27.14 | 60.78 |
| -w/o-TE | 51.35 | 40.77 | 71.68 | 38.55 | 27.26 | 61.09 |
| -w/cos | 51.38 | 41.01 | 71.51 | 38.60 | 27.32 | 60.94 |
| -w/o-init | 44.82 | 34.51 | 64.61 | 34.78 | 24.00 | 56.18 |
| -w/SiD | 51.04 | 40.56 | 71.22 | 38.13 | 26.76 | 60.73 |
| -w/WF | 51.46 | 40.87 | 71.73 | 38.55 | 27.20 | 61.06 |

analogous to relation decomposition (-w/EnD); removing the time encoder in the evolutionary dynamics encoder (-w/o-TE); replacing the proposed time encoder with cosine encoding (-w/cos); removing spatio-temporal initialization (-w/o-init); using a single decoder (-w/SiD); and applying adaptive weighted score fusion (-w/WF).

As shown in the table, we evaluate a rule-free heuristic for constructing \mathcal{G}^D (-w/Simp) by selecting the recent same-subject facts involving the query subject. Compared with -w/o- \mathcal{G}^E , this naive retrieval strategy leads to a substantial performance drop, indicating that simple temporal retrieval is insufficient for capturing informative evolutionary dynamics. Introducing entity decomposition (-w/EnD) results in slight performance degradation, suggesting that relation semantics benefit more from explicit decomposition, while entity decomposition may disrupt shared contextual information. We further analyze temporal encoding strategies in the evolutionary dynamics encoder. Removing the time encoder (-w/o-TE) significantly degrades performance, and replacing it with cosine encoding (-w/cos) yields inferior results, demonstrating the importance of explicitly modeling temporal relevance for extrapolation. Removing the spatio-temporal initialization (-w/o-init) also leads to a significant performance drop. This suggests that both historical evidence and evolutionary dynamics lack sufficient general contextual information, and that spatio-temporal initialization plays a crucial role in TKG reasoning. Compared with -w/o-(CoA & ReD), using a single decoder (-w/SiD) results in degraded performance, indicating that dual decoders enable more effective integration of conditionally non-redundant information at the prediction stage. Finally, compared with the full CHE-TKG, applying adaptive weighted score fusion (-w/WF) does not improve performance, and even leads to slightly inferior results. This may be due to the increased model complexity, which introduces additional optimization difficulty without effectively enhancing predictive signals.

E.3 Sensitivity Analysis

We experiment on ICEWS14s and ICEWS18 to analyze the effects of key hyperparameters in CHE-TKG, including the upper bound N on the number of historical facts for constructing the evolutionary dynamics graph and the contrastive alignment weight μ . Fig. 3 shows the impact of N on performance. The best results are achieved at $N = 10$ on ICEWS14s and $N = 8$ on ICEWS18. When N is too small, limited historical information hinders accurate prediction, while overly large N introduces noisy histories and increases computational cost. The smaller optimal N on ICEWS18 can be attributed to its denser event distribution and more stable evolutionary patterns. Fig. 4 illustrates the effect of μ , which controls contrastive alignment strength. Optimal performance is obtained at $\mu = 0.2$ on ICEWS14s and $\mu = 0.01$ on ICEWS18, indicating that the optimal alignment strength is dataset-dependent. In particular, ICEWS14s benefits from stronger alignment due to sparser events and less stable dynamics, whereas ICEWS18 requires weaker alignment given its denser and more stable temporal structure.

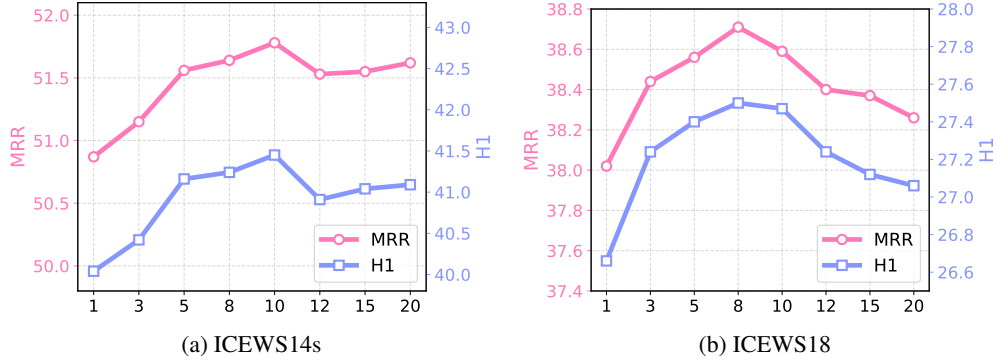


Figure 3: Effect of the upper bound N on the evolutionary dynamics graph.

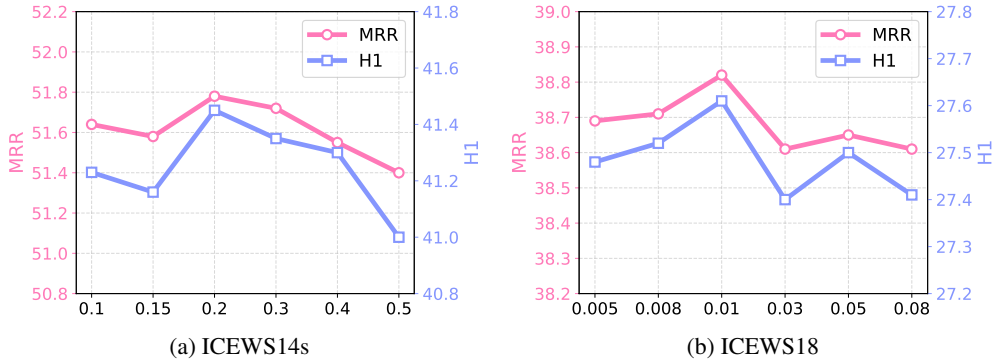


Figure 4: Effect of the contrastive alignment weight μ .

E.4 Analysis of Complementary Predictive Signals

In this subsection, we further report the signal-to-noise ratio (SNR) across different views, as shown in Table 10. Specifically, on ICEWS14s, ICEWS18, and ICEWS05-15, we observe that $\text{SNR}_{D+E} > \max\{\text{SNR}_D, \text{SNR}_E\}$, which is consistent with the condition proposed in Remark 1.

On the GDELT dataset, we find that $\text{SNR}_{D+E} > \text{SNR}_E$ while $\text{SNR}_{D+E} \approx \text{SNR}_D$. This may be attributed to the large scale of GDELT, where the margin distribution deviates from the Gaussian assumption.

Although the margin distribution in practice does not always strictly satisfy the sufficient SNR condition under the general Gaussian setting, the empirically measured pairwise ranking error still shows that score fusion effectively reduces the ranking error probability.

Table 10: Statistics on different datasets.

| Dataset | $\tilde{\gamma}_D$ | $\tilde{\gamma}_E$ | $\tilde{\gamma}_{D+E}$ | ρ_{pair} | P_{err}^D | P_{err}^E | P_{err}^{D+E} | SNR_D | SNR_E | SNR_{D+E} |
|------------|--------------------|--------------------|------------------------|----------------------|--------------------|--------------------|------------------------|----------------|----------------|--------------------|
| ICEWS14s | 7.17 | 5.78 | 12.95 | 0.723 | 0.0206 | 0.0283 | 0.0196 | 2.23 | 2.01 | 2.23 |
| ICEWS18 | 7.45 | 5.45 | 12.90 | 0.754 | 0.0151 | 0.0186 | 0.0141 | 2.49 | 2.23 | 2.53 |
| ICEWS05-15 | 8.51 | 5.24 | 13.75 | 0.724 | 0.0187 | 0.0280 | 0.0178 | 2.58 | 2.17 | 2.59 |
| GDELT | 6.28 | 3.89 | 10.17 | 0.750 | 0.0163 | 0.0203 | 0.0139 | 2.36 | 1.96 | 2.34 |

E.5 Statistical Analysis of Results

We report the standard deviation of evaluation metrics across three runs to assess the stability of our method, with all values reported in percentage form. On ICEWS14s, the standard deviations of MRR, Hits@1, and Hits@10 are 0.11, 0.13, and 0.13, respectively. On ICEWS18, the corresponding values are 0.12, 0.13, and 0.18. On ICEWS05-15, they are 0.10, 0.11, and 0.03. On GDELT, they are

Table 11: Performance comparison on ICEWS14s and ICEWS18. The best results are in **bold** and the second-best are underlined.

| Approach | ICEWS14s | | | ICEWS18 | | |
|------------|--------------|--------------|--------------|--------------|--------------|--------------|
| | MRR | Hits@1 | Hits@10 | MRR | Hits@1 | Hits@10 |
| RE-NET | 38.53 | 22.53 | <u>74.05</u> | 39.63 | 23.55 | 75.66 |
| Glean | 36.07 | 22.17 | 64.75 | 35.15 | 22.02 | 64.24 |
| RE-GCN | 40.85 | 28.15 | 68.53 | 40.68 | 27.01 | 69.51 |
| DACHA | 40.69 | 27.28 | 68.44 | 40.80 | 27.83 | 69.21 |
| TiRGN | 41.28 | 29.52 | 70.66 | 42.26 | 30.19 | 73.90 |
| EvoExplore | 28.11 | 13.97 | 57.67 | 29.82 | 18.50 | 58.01 |
| GTRL | 38.57 | 27.36 | 66.35 | 38.43 | 27.48 | 67.82 |
| DHyper | 41.71 | 29.37 | 69.32 | 42.84 | 29.96 | 70.82 |
| DECRL | 42.90 | 30.49 | 70.01 | 43.36 | 30.64 | 71.12 |
| HEDRA | 47.86 | 35.28 | 75.65 | 46.77 | 33.66 | <u>75.64</u> |
| CHE-TKG | <u>45.07</u> | <u>32.74</u> | 72.56 | <u>45.29</u> | <u>32.34</u> | <u>73.92</u> |

0.04, 0.04, and 0.01. These results demonstrate that CHE-TKG achieves stable performance across different datasets.

E.6 Relation Prediction

In Eq. 9, relation prediction is incorporated as an auxiliary objective to improve entity prediction. We further report the relation prediction performance of CHE-TKG on the ICEWS14s and ICEWS18 datasets. The compared baselines include RE-NET [19], Glean [10], RE-GCN [30], DACHA [5], TiRGN [27], EvoExplore [53], GTRL [44], DHyper [45], DECRL [6], and HEDRA [7], whose results are all taken from HEDRA [7]. As shown in the results, our method achieves the second-best performance in terms of MRR and Hits@1 on ICEWS14s, and consistently ranks second across all metrics on ICEWS18. It is worth noting that the current state-of-the-art methods are specifically designed for relation prediction, while our model is not tailored for this task. Nevertheless, CHE-TKG achieves competitive results, suggesting that it captures both entity and relational semantics effectively.

E.7 Robustness Analysis

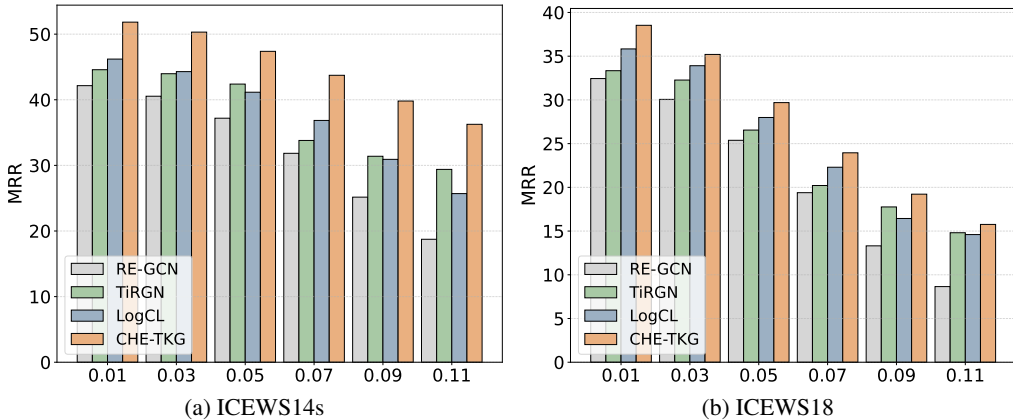


Figure 5: Robustness analysis under Gaussian noise perturbations.

We evaluate robustness by injecting Gaussian noise with varying intensities into the initial entity embeddings at inference time. We compare CHE-TKG against strong open-source baselines, includ-

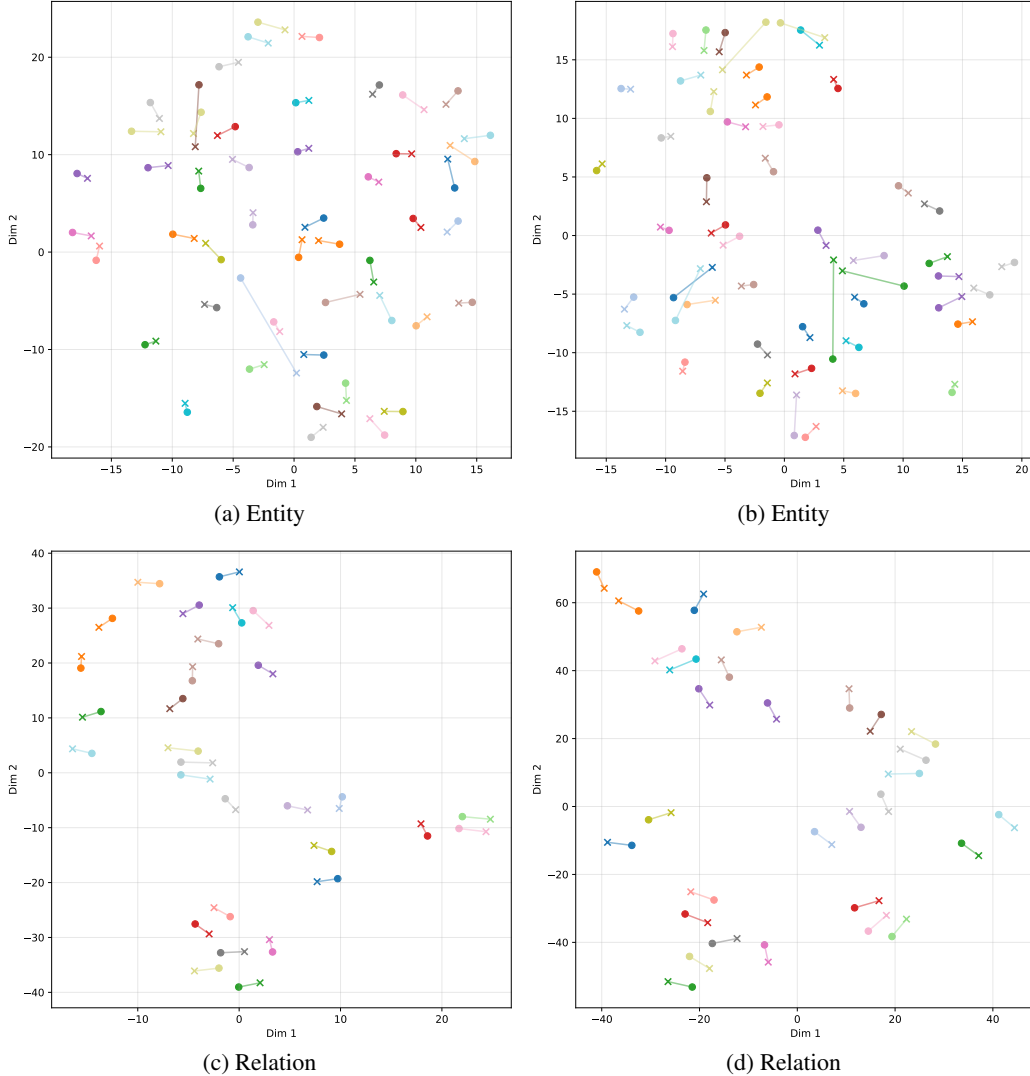


Figure 6: t-SNE visualization of entity and relation embeddings under different settings.

ing RE-GCN² [30], TiRGN³ [27], and LogCL⁴ [9]. The results are shown in Fig. 5. On ICEWS14s, CHE-TKG demonstrates the strongest robustness, exhibiting substantially smaller performance degradation as noise intensity increases. When the noise level reaches 0.11, CHE-TKG experiences an MRR drop of 30.04%, compared to 55.54% for RE-GCN and 44.37% for LogCL, indicating greater resilience to perturbations in entity representations. As analyzed in Section E.3, the evolutionary dynamics in ICEWS18 are relatively more stable, leading to smaller marginal robustness gains of CHE-TKG than those observed on ICEWS14s.

E.8 Visualization Analysis

In this subsection, we present a visualization analysis of the entity and relation representations learned by the full framework, which incorporates both relation decomposition and contrastive alignment. The results are illustrated in Fig. 6. Specifically, we apply t-SNE to visualize entity and relation embeddings from the historical evidence and evolutionary dynamics views on the ICEWS14s test set across different timestamps. We randomly select 50 entity pairs and 30 relation pairs for visualization.

²<https://github.com/Lee-zix/RE-GCN>

³<https://github.com/Liyyy2122/TiRGN>

⁴<https://github.com/WeiChen3690/LogCL>

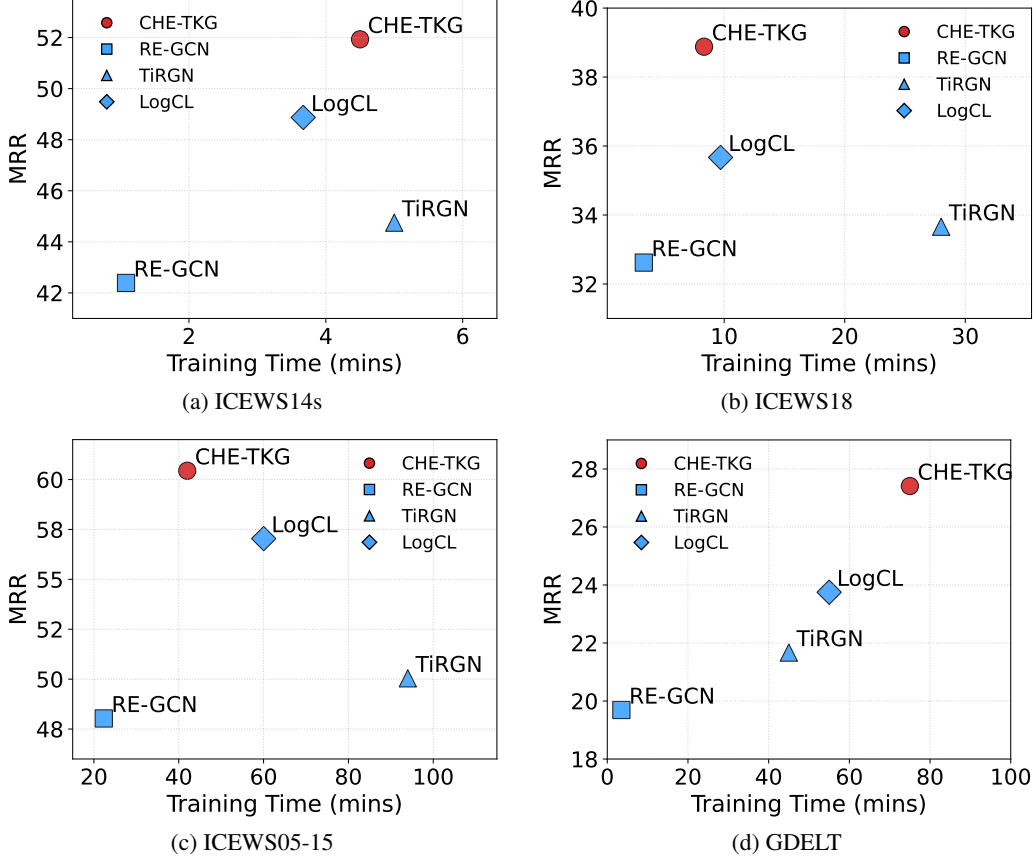


Figure 7: Efficiency-performance trade-off comparisons.

The markers “x” and “o” denote embeddings from the historical evidence view and the evolutionary dynamics view, respectively. As shown in the figure, most embeddings exhibit noticeable yet moderate shifts across the two views, indicating that the representations are not redundant. At the same time, the overall spatial structures remain largely consistent, suggesting the presence of shared information. These observations imply that the two views capture non-redundant yet correlated signals, which aligns with our assumption of conditional non-redundancy. Moreover, the structured shifts, rather than random displacements, indicate that the differences between the two views are meaningful rather than noise.

E.9 Complexity Analysis

We analyze the computational complexity of CHE-TKG from different components, omitting the embedding dimension d for clarity. For the historical evidence graph construction, the complexity is $O(|\mathcal{T}||\mathcal{F}_1|)$. For the evolutionary dynamics graph construction, we adopt temporal logical rule learning based on TLogic, with worst-case complexity $O(|\mathcal{R}|nDb)$, where n is the number of sampled walks, l is the rule length, D is the maximum node degree, and b is the number of sampled body groundings. Since l is a small constant, this term can be simplified as $O(|\mathcal{R}|nDb)$. For the temporal logical rule-based retrieval, the complexity is $O(\min(wk, N))$, which can be written as $O(N)$. For the spatio-temporal initialization module, the complexity is $O(L(|\mathcal{E}| + |\mathcal{R}| + C_{gc}))$, where C_{gc} denotes the cost of graph convolution. For the relation decomposition module, since each relation is processed independently and the embedding dimension is omitted, the complexity is $O(|\mathcal{R}|)$. For the collaborative learning stage, the HEGE and EDGE operate on query-specific subgraphs, yielding a complexity of $O(|\mathcal{E}| + |\mathcal{F}_1| + |\mathcal{F}_2|)$. For the contrastive alignment, the complexity is $O(|\mathcal{Q}_{t_q}|)$. Overall, the computational complexity of CHE-TKG is

$$O(L(|\mathcal{E}| + |\mathcal{R}| + C_{gc}) + |\mathcal{R}|nDb + |\mathcal{T}||\mathcal{F}_1| + N + |\mathcal{E}| + |\mathcal{R}| + |\mathcal{F}_1| + |\mathcal{F}_2| + |\mathcal{Q}_{t_q}|). \quad (43)$$

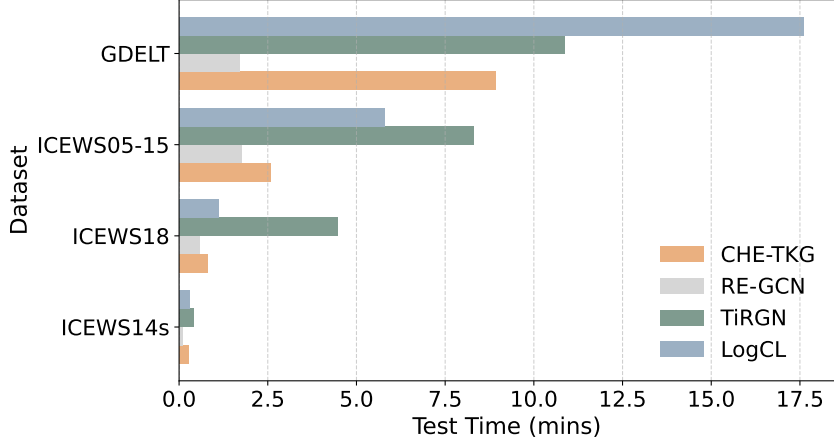


Figure 8: Test-time efficiency comparison.

E.10 Execution Time Analysis

We analyze the efficiency and predictive performance of CHE-TKG against strong open-source baselines, including RE-GCN [30], TiRGN [27], and LogCL [9], as shown in Fig. 7. Here, training time is measured as the time per epoch. On all datasets, CHE-TKG achieves a favorable balance between efficiency and performance. Compared with RE-GCN, CHE-TKG incurs moderately higher training time but consistently yields substantially better MRR. In contrast, more complex methods such as TiRGN and LogCL exhibit significantly higher training costs but underperform CHE-TKG. These results demonstrate that CHE-TKG provides an effective trade-off between computational efficiency and extrapolation accuracy. Despite encoding both historical evidence and evolutionary dynamics graphs, efficient spatio-temporal initialization with a limited number of recent snapshots enables CHE-TKG to achieve strong performance without excessive overhead. On the GDELT dataset, our method incurs slightly higher training time than all baselines, likely due to the use of GAT. In addition, CHE-TKG incurs only slightly higher testing time than the simple baseline RE-GCN, but is more efficient than TiRGN and LogCL across ICEWS14s, ICEWS18, ICEWS05-15, and GDELT, as shown in Fig. 8.

F Additional Details on Initialization

Following prior work [29, 54, 9], we incorporate temporal encoding in the initialization stage to model temporal evolution and periodic patterns.

Given the relative timestamp $\tau = t_q - t_i$, we compute a cosine-based temporal encoding:

$$\phi(\tau) = \cos(w_\tau \tau + b_\tau), \quad (44)$$

where w_τ and b_τ are learnable parameters.

The temporal encoding is concatenated with the entity embedding and projected as:

$$\mathbf{e}_t = W_0 [\mathbf{e}_i \parallel \phi(\tau)], \quad (45)$$

where $[\cdot \parallel \cdot]$ denotes concatenation and $W_0 \in \mathbb{R}^{d \times 2d}$ is a linear projection matrix.

The resulting representation \mathbf{e}_t is then used as the input to the GNN in the initialization stage.

G Limitations and Broader Impacts

G.1 Limitations

Although our method improves entity extrapolation performance on benchmark datasets by explicitly modeling historical evidence and evolutionary dynamics, it still has several limitations. In particular, it

remains unclear which neighborhoods in the historical evidence graph and the evolutionary dynamics graph contribute most to TKGR, limiting the interpretability of CHE-TKG and calling for further investigation.

G.2 Broader Impacts

CHE-TKG provides a framework for predicting future facts in temporal knowledge graphs, which can support future-oriented reasoning in applications such as event forecasting, recommendation, risk monitoring, and decision support. By jointly modeling historical evidence and evolutionary dynamics, it may help identify plausible future links and provide useful signals for downstream analysis. However, predictions from CHE-TKG should be used with caution, especially in high-stakes domains. Since the model relies on historical data, it may inherit biases, noise, or incompleteness from the observed knowledge graph. Potential misuse, such as inferring sensitive relationships or supporting surveillance-oriented applications, should also be considered. Therefore, CHE-TKG should be used as a decision-support tool with appropriate human oversight, data governance, and ethical safeguards.

NeurIPS Paper Checklist

1. Claims

Question: Do the main claims made in the abstract and introduction accurately reflect the paper’s contributions and scope?

Answer: [Yes]

Justification: The abstract and introduction include claims that accurately reflect the paper’s contributions and scope.

Guidelines:

- The answer [N/A] means that the abstract and introduction do not include the claims made in the paper.
- The abstract and/or introduction should clearly state the claims made, including the contributions made in the paper and important assumptions and limitations. A [No] or [N/A] answer to this question will not be perceived well by the reviewers.
- The claims made should match theoretical and experimental results, and reflect how much the results can be expected to generalize to other settings.
- It is fine to include aspirational goals as motivation as long as it is clear that these goals are not attained by the paper.

2. Limitations

Question: Does the paper discuss the limitations of the work performed by the authors?

Answer: [Yes]

Justification: The limitations of this work are discussed in Appendix G.1.

Guidelines:

- The answer [N/A] means that the paper has no limitation while the answer [No] means that the paper has limitations, but those are not discussed in the paper.
- The authors are encouraged to create a separate “Limitations” section in their paper.
- The paper should point out any strong assumptions and how robust the results are to violations of these assumptions (e.g., independence assumptions, noiseless settings, model well-specification, asymptotic approximations only holding locally). The authors should reflect on how these assumptions might be violated in practice and what the implications would be.
- The authors should reflect on the scope of the claims made, e.g., if the approach was only tested on a few datasets or with a few runs. In general, empirical results often depend on implicit assumptions, which should be articulated.
- The authors should reflect on the factors that influence the performance of the approach. For example, a facial recognition algorithm may perform poorly when image resolution is low or images are taken in low lighting. Or a speech-to-text system might not be used reliably to provide closed captions for online lectures because it fails to handle technical jargon.
- The authors should discuss the computational efficiency of the proposed algorithms and how they scale with dataset size.
- If applicable, the authors should discuss possible limitations of their approach to address problems of privacy and fairness.
- While the authors might fear that complete honesty about limitations might be used by reviewers as grounds for rejection, a worse outcome might be that reviewers discover limitations that aren’t acknowledged in the paper. The authors should use their best judgment and recognize that individual actions in favor of transparency play an important role in developing norms that preserve the integrity of the community. Reviewers will be specifically instructed to not penalize honesty concerning limitations.

3. Theory assumptions and proofs

Question: For each theoretical result, does the paper provide the full set of assumptions and a complete (and correct) proof?

Answer: [Yes]

Justification: Theorem 1 provides the full assumptions and correct derivations, with the proof included in Appendix D. We also empirically verify the assumptions in Section 4.5.

Guidelines:

- The answer [N/A] means that the paper does not include theoretical results.
- All the theorems, formulas, and proofs in the paper should be numbered and cross-referenced.
- All assumptions should be clearly stated or referenced in the statement of any theorems.
- The proofs can either appear in the main paper or the supplemental material, but if they appear in the supplemental material, the authors are encouraged to provide a short proof sketch to provide intuition.
- Inversely, any informal proof provided in the core of the paper should be complemented by formal proofs provided in appendix or supplemental material.
- Theorems and Lemmas that the proof relies upon should be properly referenced.

4. Experimental result reproducibility

Question: Does the paper fully disclose all the information needed to reproduce the main experimental results of the paper to the extent that it affects the main claims and/or conclusions of the paper (regardless of whether the code and data are provided or not)?

Answer: [Yes]

Justification: The paper provides all necessary information to reproduce the main experimental results.

Guidelines:

- The answer [N/A] means that the paper does not include experiments.
- If the paper includes experiments, a [No] answer to this question will not be perceived well by the reviewers: Making the paper reproducible is important, regardless of whether the code and data are provided or not.
- If the contribution is a dataset and/or model, the authors should describe the steps taken to make their results reproducible or verifiable.
- Depending on the contribution, reproducibility can be accomplished in various ways. For example, if the contribution is a novel architecture, describing the architecture fully might suffice, or if the contribution is a specific model and empirical evaluation, it may be necessary to either make it possible for others to replicate the model with the same dataset, or provide access to the model. In general, releasing code and data is often one good way to accomplish this, but reproducibility can also be provided via detailed instructions for how to replicate the results, access to a hosted model (e.g., in the case of a large language model), releasing of a model checkpoint, or other means that are appropriate to the research performed.
- While NeurIPS does not require releasing code, the conference does require all submissions to provide some reasonable avenue for reproducibility, which may depend on the nature of the contribution. For example
 - (a) If the contribution is primarily a new algorithm, the paper should make it clear how to reproduce that algorithm.
 - (b) If the contribution is primarily a new model architecture, the paper should describe the architecture clearly and fully.
 - (c) If the contribution is a new model (e.g., a large language model), then there should either be a way to access this model for reproducing the results or a way to reproduce the model (e.g., with an open-source dataset or instructions for how to construct the dataset).
 - (d) We recognize that reproducibility may be tricky in some cases, in which case authors are welcome to describe the particular way they provide for reproducibility. In the case of closed-source models, it may be that access to the model is limited in some way (e.g., to registered users), but it should be possible for other researchers to have some path to reproducing or verifying the results.

5. Open access to data and code

Question: Does the paper provide open access to the data and code, with sufficient instructions to faithfully reproduce the main experimental results, as described in supplemental material?

Answer: [Yes]

Justification: The paper provides anonymized code, including training and evaluation code, environment setup, execution commands, and the code, environment, and commands used for graph construction.

Guidelines:

- The answer [N/A] means that paper does not include experiments requiring code.
- Please see the NeurIPS code and data submission guidelines (<https://neurips.cc/public/guides/CodeSubmissionPolicy>) for more details.
- While we encourage the release of code and data, we understand that this might not be possible, so [No] is an acceptable answer. Papers cannot be rejected simply for not including code, unless this is central to the contribution (e.g., for a new open-source benchmark).
- The instructions should contain the exact command and environment needed to run to reproduce the results. See the NeurIPS code and data submission guidelines (<https://neurips.cc/public/guides/CodeSubmissionPolicy>) for more details.
- The authors should provide instructions on data access and preparation, including how to access the raw data, preprocessed data, intermediate data, and generated data, etc.
- The authors should provide scripts to reproduce all experimental results for the new proposed method and baselines. If only a subset of experiments are reproducible, they should state which ones are omitted from the script and why.
- At submission time, to preserve anonymity, the authors should release anonymized versions (if applicable).
- Providing as much information as possible in supplemental material (appended to the paper) is recommended, but including URLs to data and code is permitted.

6. Experimental setting/details

Question: Does the paper specify all the training and test details (e.g., data splits, hyperparameters, how they were chosen, type of optimizer) necessary to understand the results?

Answer: [Yes]

Justification: The paper provides the training and test details in Appendix E.1.

Guidelines:

- The answer [N/A] means that the paper does not include experiments.
- The experimental setting should be presented in the core of the paper to a level of detail that is necessary to appreciate the results and make sense of them.
- The full details can be provided either with the code, in appendix, or as supplemental material.

7. Experiment statistical significance

Question: Does the paper report error bars suitably and correctly defined or other appropriate information about the statistical significance of the experiments?

Answer: [Yes]

Justification: The paper provides information about the statistical significance of the experiments in Appendix E.5.

Guidelines:

- The answer [N/A] means that the paper does not include experiments.
- The authors should answer [Yes] if the results are accompanied by error bars, confidence intervals, or statistical significance tests, at least for the experiments that support the main claims of the paper.
- The factors of variability that the error bars are capturing should be clearly stated (for example, train/test split, initialization, random drawing of some parameter, or overall run with given experimental conditions).

- The method for calculating the error bars should be explained (closed form formula, call to a library function, bootstrap, etc.)
- The assumptions made should be given (e.g., Normally distributed errors).
- It should be clear whether the error bar is the standard deviation or the standard error of the mean.
- It is OK to report 1-sigma error bars, but one should state it. The authors should preferably report a 2-sigma error bar than state that they have a 96% CI, if the hypothesis of Normality of errors is not verified.
- For asymmetric distributions, the authors should be careful not to show in tables or figures symmetric error bars that would yield results that are out of range (e.g., negative error rates).
- If error bars are reported in tables or plots, the authors should explain in the text how they were calculated and reference the corresponding figures or tables in the text.

8. Experiments compute resources

Question: For each experiment, does the paper provide sufficient information on the computer resources (type of compute workers, memory, time of execution) needed to reproduce the experiments?

Answer: [Yes]

Justification: The paper provides the compute resources used for the experiments in Appendix E.1.

Guidelines:

- The answer [N/A] means that the paper does not include experiments.
- The paper should indicate the type of compute workers CPU or GPU, internal cluster, or cloud provider, including relevant memory and storage.
- The paper should provide the amount of compute required for each of the individual experimental runs as well as estimate the total compute.
- The paper should disclose whether the full research project required more compute than the experiments reported in the paper (e.g., preliminary or failed experiments that didn't make it into the paper).

9. Code of ethics

Question: Does the research conducted in the paper conform, in every respect, with the NeurIPS Code of Ethics <https://neurips.cc/public/EthicsGuidelines>?

Answer: [Yes]

Justification: The research conducted in this paper conforms to the NeurIPS Code of Ethics in all aspects, including data collection, experimental design, and result dissemination, and involves no ethical violations or risks.

Guidelines:

- The answer [N/A] means that the authors have not reviewed the NeurIPS Code of Ethics.
- If the authors answer [No], they should explain the special circumstances that require a deviation from the Code of Ethics.
- The authors should make sure to preserve anonymity (e.g., if there is a special consideration due to laws or regulations in their jurisdiction).

10. Broader impacts

Question: Does the paper discuss both potential positive societal impacts and negative societal impacts of the work performed?

Answer: [Yes]

Justification: The paper discusses the potential societal impacts of this work in Appendix G.2.

Guidelines:

- The answer [N/A] means that there is no societal impact of the work performed.

- If the authors answer [N/A] or [No], they should explain why their work has no societal impact or why the paper does not address societal impact.
- Examples of negative societal impacts include potential malicious or unintended uses (e.g., disinformation, generating fake profiles, surveillance), fairness considerations (e.g., deployment of technologies that could make decisions that unfairly impact specific groups), privacy considerations, and security considerations.
- The conference expects that many papers will be foundational research and not tied to particular applications, let alone deployments. However, if there is a direct path to any negative applications, the authors should point it out. For example, it is legitimate to point out that an improvement in the quality of generative models could be used to generate Deepfakes for disinformation. On the other hand, it is not needed to point out that a generic algorithm for optimizing neural networks could enable people to train models that generate Deepfakes faster.
- The authors should consider possible harms that could arise when the technology is being used as intended and functioning correctly, harms that could arise when the technology is being used as intended but gives incorrect results, and harms following from (intentional or unintentional) misuse of the technology.
- If there are negative societal impacts, the authors could also discuss possible mitigation strategies (e.g., gated release of models, providing defenses in addition to attacks, mechanisms for monitoring misuse, mechanisms to monitor how a system learns from feedback over time, improving the efficiency and accessibility of ML).

11. Safeguards

Question: Does the paper describe safeguards that have been put in place for responsible release of data or models that have a high risk for misuse (e.g., pre-trained language models, image generators, or scraped datasets)?

Answer: [N/A]

Justification: The paper does not involve the release of data or models with a high risk for misuse.

Guidelines:

- The answer [N/A] means that the paper poses no such risks.
- Released models that have a high risk for misuse or dual-use should be released with necessary safeguards to allow for controlled use of the model, for example by requiring that users adhere to usage guidelines or restrictions to access the model or implementing safety filters.
- Datasets that have been scraped from the Internet could pose safety risks. The authors should describe how they avoided releasing unsafe images.
- We recognize that providing effective safeguards is challenging, and many papers do not require this, but we encourage authors to take this into account and make a best faith effort.

12. Licenses for existing assets

Question: Are the creators or original owners of assets (e.g., code, data, models), used in the paper, properly credited and are the license and terms of use explicitly mentioned and properly respected?

Answer: [Yes]

Justification: The paper properly cites the existing datasets and open-source code used in this work and respects their licenses and terms of use.

Guidelines:

- The answer [N/A] means that the paper does not use existing assets.
- The authors should cite the original paper that produced the code package or dataset.
- The authors should state which version of the asset is used and, if possible, include a URL.
- The name of the license (e.g., CC-BY 4.0) should be included for each asset.

- For scraped data from a particular source (e.g., website), the copyright and terms of service of that source should be provided.
- If assets are released, the license, copyright information, and terms of use in the package should be provided. For popular datasets, paperswithcode.com/datasets has curated licenses for some datasets. Their licensing guide can help determine the license of a dataset.
- For existing datasets that are re-packaged, both the original license and the license of the derived asset (if it has changed) should be provided.
- If this information is not available online, the authors are encouraged to reach out to the asset's creators.

13. **New assets**

Question: Are new assets introduced in the paper well documented and is the documentation provided alongside the assets?

Answer: [Yes]

Justification: The paper provides anonymized code for training, and no new dataset is released.

Guidelines:

- The answer [N/A] means that the paper does not release new assets.
- Researchers should communicate the details of the dataset/code/model as part of their submissions via structured templates. This includes details about training, license, limitations, etc.
- The paper should discuss whether and how consent was obtained from people whose asset is used.
- At submission time, remember to anonymize your assets (if applicable). You can either create an anonymized URL or include an anonymized zip file.

14. **Crowdsourcing and research with human subjects**

Question: For crowdsourcing experiments and research with human subjects, does the paper include the full text of instructions given to participants and screenshots, if applicable, as well as details about compensation (if any)?

Answer: [N/A]

Justification: The paper does not involve crowdsourcing or research with human subjects.

Guidelines:

- The answer [N/A] means that the paper does not involve crowdsourcing nor research with human subjects.
- Including this information in the supplemental material is fine, but if the main contribution of the paper involves human subjects, then as much detail as possible should be included in the main paper.
- According to the NeurIPS Code of Ethics, workers involved in data collection, curation, or other labor should be paid at least the minimum wage in the country of the data collector.

15. **Institutional review board (IRB) approvals or equivalent for research with human subjects**

Question: Does the paper describe potential risks incurred by study participants, whether such risks were disclosed to the subjects, and whether Institutional Review Board (IRB) approvals (or an equivalent approval/review based on the requirements of your country or institution) were obtained?

Answer: [N/A]

Justification: The paper does not involve crowdsourcing or research with human subjects.

Guidelines:

- The answer [N/A] means that the paper does not involve crowdsourcing nor research with human subjects.

- Depending on the country in which research is conducted, IRB approval (or equivalent) may be required for any human subjects research. If you obtained IRB approval, you should clearly state this in the paper.
- We recognize that the procedures for this may vary significantly between institutions and locations, and we expect authors to adhere to the NeurIPS Code of Ethics and the guidelines for their institution.
- For initial submissions, do not include any information that would break anonymity (if applicable), such as the institution conducting the review.

16. Declaration of LLM usage

Question: Does the paper describe the usage of LLMs if it is an important, original, or non-standard component of the core methods in this research? Note that if the LLM is used only for writing, editing, or formatting purposes and does *not* impact the core methodology, scientific rigor, or originality of the research, declaration is not required.

Answer: [N/A]

Justification: The core method development in this research does not involve LLMs as important, original, or non-standard components.

Guidelines:

- The answer [N/A] means that the core method development in this research does not involve LLMs as any important, original, or non-standard components.
- Please refer to our LLM policy in the NeurIPS handbook for what should or should not be described.